applied sciences

IMPACT FACTOR 2.838

CITESCORE 3.7

Review

Colon Delivery of Nutraceutical Ingredients by Food-Grade Polymeric Systems: An Overview of Technological Characterization and Biological Evaluation

Salvatore Rizzo, Elide Zingale, Alessia Romeo, Rosamaria Lombardo and Rosario Pignatello

Special Issue

Advanced Materials and Technologies for Modified Drug Release Systems

Edited by

Prof. Dr. Rosario Pignatello and Prof. Dr. Cinzia Anna Ventura

MDPI

https://doi.org/10.3390/app13095443

applied sciences

MDPI

Review

Colon Delivery of Nutraceutical Ingredients by Food-Grade Polymeric Systems: An Overview of Technological Characterization and Biological Evaluation

Salvatore Rizzo [1], Elide Zingale [1,2], Alessia Romeo [1], Rosamaria Lombardo [1] and Rosario Pignatello [1,2,3,*]

[1] Department of Pharmaceutical and Health Sciences, University of Catania, 95125 Catania, Italy; salvo_rizzo@outlook.it (S.R.); elide.zingale@gmail.com (E.Z.); alessia.romeo@phd.unict.it (A.R.); rosamaria.lombardo@phd.unict.it (R.L.)
[2] CERNUT—Interdepartmental Research Center on Nutraceuticals and Health Products, University of Catania, 95125 Catania, Italy
[3] NANOMED—Research Center on Nanomedicine and Pharmaceutical Nanotechnology, University of Catania, 95125 Catania, Italy
* Correspondence: rosario.pignatello@unict.it

Featured Application: Design and development of smart food supplements and fortified foods for colon-targeted delivery of pre- and probiotics, nutraceuticals, and other bioactive agents.

Abstract: The development of food-grade carriers based on EFSA and/or FDA-approved polymeric materials is an area of growing interest for the targeted delivery of bioactive compounds to the colon. Many nutraceuticals have shown promise in the local treatment of conditions that threaten quality of life, such as ulcerative colitis, Crohn's disease, colorectal cancer, dysbiosis and other problems affecting the gut and colon. Nevertheless, their bioavailability is often limited due to poor solubility, rapid metabolism and low permeability, as well as undesirable local side effects. Encapsulation in carriers, which can protect the active ingredient from degradation and improve absorption and targeted administration in the colon, is one way to overcome these limitations. The technological characterization of these systems is important to assess their efficacy, safety and stability. In particular, morphology, size and surface properties influence their actions and interaction with the bio-phase. Meanwhile, encapsulation efficiency, profile and in vitro release kinetics are key parameters to assess the ability to reach the target site. This paper proposes a recent review of food-grade polymer-based systems for colorectal targeting of bioactive substances, focusing on their technological characterization and assessment of stability and biological activity, which are important in determining their full bench-to-bed potential.

Keywords: IBS; IBD; gastro-intestinal diseases; nanomedicine; microparticles; biopolymers; food supplements; chitosan; zein; pectin; alginate; inulin; Eudraguard®; shellac

Citation: Rizzo, S.; Zingale, E.; Romeo, A.; Lombardo, R.; Pignatello, R. Colon Delivery of Nutraceutical Ingredients by Food-Grade Polymeric Systems: An Overview of Technological Characterization and Biological Evaluation. *Appl. Sci.* **2023**, *13*, 5443. https://doi.org/10.3390/app13095443

Academic Editor: Antonio Valero

Received: 17 March 2023
Revised: 12 April 2023
Accepted: 21 April 2023
Published: 27 April 2023

1. Introduction

For the treatment of inflammatory bowel diseases (IBD) including ulcerative colitis (UC) and Crohn's disease (CD), colorectal cancer and adenocarcinoma, dysbiosis and other local inflammatory conditions (IBS), colon-targeted drug delivery methods can offer several advantages [1,2]. For example, they can facilitate local treatment of affections by delivering the active ingredient directly to the target site, avoiding systemic absorption and reducing possible side effects. In addition, they can enable the delivery of peptides and proteins with therapeutic activity by protecting them from enzymatic degradation and denaturation processes caused by the adverse environment and the strong pH variations between stomach and small intestine. Oral colon therapy shows high therapeutic adherence by patients. It is safe and does not require sterile production conditions. It also has economic advantages due to low production costs.

However, it still presents some challenges. As the colon is the most distal part of the gastrointestinal tract (GIT), it is difficult to ensure that the administered dose of drug reaches the colon in its entirety as it may undergo degradation and/or absorption processes in the stomach and small intestine. In fact, the enzymes present along the GIT and the extremely low pH conditions of the stomach can easily degrade sensitive bioactive substances. Different types of natural, synthetic and semi-synthetic polymers have been studied to overcome the strong physiological variations in the upper part of the GIT and ensure drug release in the colon [3–5]. Such polymers can be used to develop a variety of delivery systems, i.e., from classical matrix tablets to more complex and sophisticated osmotic pressure drug delivery systems. These exploit the peculiar conditions of the intestinal area such as pH variations, presence of enzymes or bacterial metabolic activity, biochemical pathways, time and pressure [1,6,7]. Undoubtedly, more advanced technologies represent a promising approach for colon-specific drug delivery, e.g., microspheres, nanoparticles, liposomes, mini-capsules, and mini-tablets. These have demonstrated not only a good ability to deliver the drug in the colon but also to release it in a prolonged manner [6].

Among the most widely used polymer materials, those for food-grade use are of increasing interest. These are polymers approved for food applications by government authorities (EFSA for EU and FDA for USA) for their properties such as low toxicity, biocompatibility and biodegradability. Moreover, from an industrial point of view, they have low production costs and easy availability. Due to these numerous advantages, the scientific community has shown considerable interest in their use in the development of modified delivery systems not only for drugs, but also for nutraceuticals, pro- and prebiotics, phytoextracts, phytotherapeutics, and other natural biomolecules. The interest is in the potential use of modified delivery systems for highly biocompatible and biodegradable colon-specific drugs, as well as in the development of smart food supplements and new fortified foods useful or adjuvant to conventional therapy against major colon disorders [8–11].

Recent reviews have discussed the topic of colon-targeted delivery systems based on food polymers. Zhang et al. focused on the delivery of polyphenols through platforms based on food biopolymers (proteins and commercial polysaccharides), analyzing their design, production and use [8]. The design is obviously aimed at systems that improve the physicochemical properties, stability, bioavailability, and biological activity of polyphenols. It has been shown that the use of several polyphenols in one delivery system can generate more effective functional foods by exploiting the synergistic effects produced. However, the design and use of such co-delivery systems have posed many challenges, including the need to improve the taste and mitigate the astringency of some polyphenols. In addition, further in vitro and in vivo studies should be conducted to evaluate the efficacy and potential toxicity of polyphenol combinations, and a systematic study of the behavior of these delivery systems in the context of commercial foods and beverages. Finally, a deeper understanding of the design and functioning of single or multiple polyphenol delivery systems could lead to the creation of new products that can be used in the food, supplement and pharmaceutical industries [8]. Kumar et al. developed mucoadhesive carriers based on food-grade polymers such as chitosan, alginate and pectin for the delivery of drugs to the colon [9]. Due to their ability to overcome gastric fluid and mucoadhesive properties, these systems are able to adhere to mucus and facilitate the effective absorption of poorly soluble substances delivered. Moreover, modulation of the release of chemotherapeutic agents has made it possible to reduce or eliminate their side effects. Thus, they present great potential for the development of next-generation personalized medicine platforms. However, the absence of an ex vivo experimental model to be able to carry out more in-depth studies (physicochemical interactions, toxicological aspects, etc.) of the potential of these systems and the gap between academic research and clinical application are the main obstacles to their development [9]. Bakshi et al. focused on exploiting the metabolism of the gut microbiome for targeted colon drug delivery. The different delivery systems and modulation of the microbiota are highlighted. The potential of using bacteria for the production of therapeutic molecules is also discussed. In particular, the manipulation of gut bacteria to express specific enzymes that activate drugs for the treatment of certain types of cancer. However, there are few

in vitro, in vivo and clinical studies to evaluate the current experimental evidence. Therefore, an increase in such studies and research aimed at determining the consequences of microbial metabolism of these drugs (in relation to their efficacy and toxicity) in various pathological conditions of the colon is of enormous interest [10]. Finally, Ibrahim reviewed the advances in polysaccharide-based oral colon delivery systems, highlighting the possibility of creating delivery platforms that are unaffected by the gastric environment and are selectively digested by colon bacterial enzymes. Unfortunately, during disease states, a dilution and/or change in the bacterial population occurs, which is the main challenge of this administration approach. Co-administration of probiotics could compensate for the bacterial loss. However, this research is limited to the preclinical level and further studies are needed for industrial scalability and clinical use of these technologies [11].

This review focuses on technological and biological characterization studies of the most recent total food systems proposed for colon-targeted delivery. The main characteristic of these systems is the nature of their components: all their components are considered food or food additives approved for human use. The review is the result of an extensive screening process of numerous articles identified on PubMed, Google Scholar, SciELO and ScienceDirect platforms, setting the last 5 years as the timeframe and using as keywords: colon targeting, food polymers in colon-targeting, resveratrol, quercetin and other nutraceuticals, IBD, ulcerative colitis, Crohn's disease, colorectal cancer, and other colon disorders. The objective screening phase made it possible to significantly reduce sources, identifying only those studies that fell within the previously provided definition of total food-grade colon-targeting systems, preferring, where possible, studies based on eco-friendly production processes.

2. Food-Grade Polymers

The use of food-grade polymers (Figure 1) for colon targeting allows the development of systems for the controlled delivery of active and health-beneficial substances (nutraceuticals, prebiotics, probiotics, etc.) to the ileo-colon section tract against GIT diseases (IBD, IBS, colon cancer, dysbiosis and other conditions) with a high safety profile [12]. In fact, food-grade polymers are approved for use in the food industry and are safe for human consumption. In the development of controlled-release systems, they are often used in combination to obtain systems capable of resisting stomach acidity and hydrolysis by intestinal enzymes, and then ensuring the release of the substance delivered into the colon through different mechanisms (dissolution/erosion, pH- or time-dependent swelling or degradation, hydrolysis mediated by specific enzymes produced by the colonic bacterial flora, etc.) [1,2,6,7].

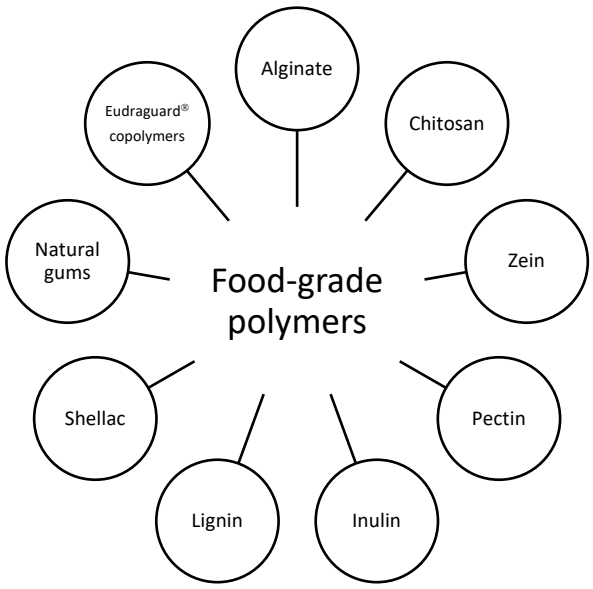

Figure 1. An overview of the most used food-grade polymers.

Table 1 gathers some physicochemical properties of the polymers that will be further investigated for their applications in colon-targeted food products.

2.1. Alginates

Widely used for the development of these systems is **alginate** (E400), an asymmetric block polymer of mannuronic acid and guluronic acid (in varying proportions) (Figure 2). It can be obtained by extraction from brown algae in salt form by treatment in an alkaline environment or by bacterial fermentation (*Azotobacter* and *Pseudomonas*).

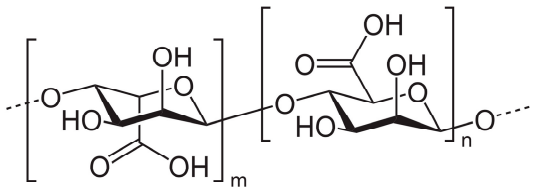

Figure 2. Monomeric structure of alginate.

Due to its properties (excellent biocompatibility, low cost, inert nature, chemical compatibility and easy availability), it has been used for the development of various systems, including microspheres that enable the encapsulation of small and large molecules with different chemical properties.

Among the preparation methods of these systems, the most widely used is the ionotropic method, which involves the use of Ca^{2+} cations to gel transition an alginate solution [45]. The drug release mechanism depends on its ability to swell as a function of pH. In fact, at neutral pH, pore enlargement of the gel structure occurs. Yu et al. developed uniform-shell microparticles for protein delivery using a microfluidic approach. By encapsulating inulin and coating the microparticles with chitosan, the system allowed minimal release for 5 days in an acidic environment (pH 3) and then accelerated to pH 7. The inulin allowed for reduced pore enlargement of the alginate network at pH 7 (similarly to pore plugs), slowing the release of OVA, which in turn was further controlled by the presence of chitosan coating [46].

2.2. Chitosans

Another interesting polysaccharide is **chitosan** (Commission Regulation (EU) 2016/355 of 11 March 2016). It is produced by chemical deacetylation of chitin, the second most abundant polysaccharide after cellulose. Both chitin and chitosan are found in the shells of crustaceans and aquatic microorganisms (such as crabs or shrimp), in the cell walls of fungi, and in the exoskeleton (or wings) of insects. Structurally, chitosan is a linear polysaccharide consisting of randomly distributed D-glucosamine (deacetylated unit) and N-acetyl-D-glucosamine (acetylated unit) and β-(1→4) bonds (Figure 3). Its molecular weight ranges from 50 to 1000 kDa, with a deacetylation degree of 30–95%, depending on the source and processing method. Both parameters determine the properties and mode of action of chitosan in biological systems. It has a positive surface charge (free amine groups) and acidic aqueous solubility. Moreover, it is characterized by a high plasticity that allows its use in the preparation of, for example, transparent, flexible, nanostructured and self-assembled films, nanofibers, microspheres and porous hydrogels [47–49].

A recent work by Tie et al. described a microfluidic approach to produce pH-controlled release systems of procyanidins (PCs) containing chitosan and alginate with a retention rate of 86% in aqueous solution for 168 h. The study showed a reduction in the size of microparticles in simulated gastric fluid (SGF) (compared with salivary fluid), probably due to contraction of the alginate gel. However, their breakdown in simulated intestinal fluid (SIF) (pH 7.4), resulting in cargo release, confirmed their potential use as a colon-targeted delivery system [50].

Table 1. Main physicochemical properties of food-grade polymers.

Polymer (CAS Number)	Ave. MW Range (kDa)	Solubility	WVP and MA	Isoelectric Point (pH)	Thermal Behavior (°C) (a) Tg (b) Tm (c) Td	Color	Odor	Flavor	Origin	Refs.
Alginate (9005-38-3)	51–173	Soluble in water. Insoluble in alcohol, chloroform and ether	WVP = 6.16 × 10–7 MA = 60%	5.4	(a) 212 (b) 99 (c) ≥300	White-light beige	Odorless	None	Salt of alginic acid derived by brown algae	[13–16]
Inulin (9005-80-5)	0.6–7	Water (moderately soluble at 25 °C, soluble at 80 °C); ethanol: almost insoluble	WVP = 4.3 MA = 12–15 g/100 g dry inulin	5–7	(a) 175 (b)140–180 § (c)190–220 §	White	Odorless	None	Chicory roots	[17–21]
Chitosan (9012-76-4)	150–600	Soluble at pH ≤ 6	WVP = 3.64–6.56 MA = 7–11%	~9	(a) ~203 (medium Mw chitosan) (b) 290 (medium Mw chitosan) (c) 380	White or almost white fine powder	Fishy odor	Astringent taste	Linear polysaccharide derived from crustacean exoskeleton	[22–25]
Pectin (9000-69-5)	50–150	Soluble in water	WVP = 4.47 MA = 48.55%	3.5	(a) 16.8 to −24.6 (depending on water content) (b) 174–180 (c) ≥100 (pH-based)	From with to light brown powder	Odorless	None	Fruits (pears, apples, plums, gooseberries) and citrus fruits (oranges)	[26–29]
α-Zein **(9010-66-6)**	22–24	Soluble in ethanol (60–95%) and in alkaline aqueous solutions (pH ≥ 11)	WVP = ~0.13 MA ≤ 8%	6.2	(a) 93 (b) 80–87 (c) 280	Yellowish	Odorless	None	Cereal seeds and maize	[30–32]
Almond gum	15.9×10^3	Soluble in water, insoluble in organic solvents, glycerin, paraffin oil	WVP = 18 MA = 14.89%	4.5–5.5	(a) 58.5 (b) 174 (c) 410	Light brown or pale yellow	Odorless	None	Produced by almond trees	[33–37]
Gellan gum (71010-52-1)	500	Hot water (>70 °C)	WVP = 16.8 MA = ~28%	4.5	(a) ~70–80 (b) n.a. (c) >80	White	Odorless	None	Produced by Pseudomonas elodea	[38,39]
Eudra-guard Biotic (26936-24-3)	280	pH-dependent water-solubility (soluble above pH 7); soluble in acetone, ethanol and isopropyl alcohol	/	/	(a) 48	White	Odorless	None	Synthetic methacrylate copolymer	[40,41]
Eudra-guard Control (9010-88-2)	600	Soluble in acetone, ethanol and isopropyl alcohol. Miscible with water.	/	/	n.a.	White	Odorless	None	Synthetic methacrylate copolymer	[40]
Shellac (gum) (9000-59-3)	0.58	Soluble in ethyl alcohol		4.6	(b) 75	Yellow (from blonde color to dark brown)	pretty strong smell—mild alcohol odor	Bitter taste	Refined from a resinous substance excreted by an insect (Laccifer lacca)	[42]
Lignin (8068-05-1)	≥5	Poorly soluble in water; soluble in methanol and dioxane	MA = 0.59%		(a) 90 (b) 170	From black to brown as pH decreases	smoky or sulfurous smell	None	Derived mainly from hydroxy-cinnamyl alcohols	[43,44]

WVP, water vapor permeability (expressed as g. mm/m^2. h. kPa); MA, moisture absorption; Tg, glass transition temperature; Tm, melting point; Td, thermal degradation point. § Values largely vary in literature based on different plant origin of inulins.

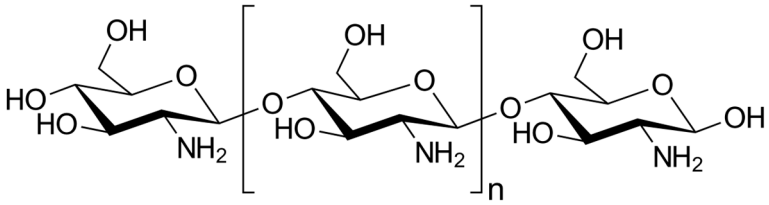

Figure 3. General structure of chitosans.

2.3. Zein

Zein is another macromolecule with interesting self-assembling properties for biomedical applications, drug delivery and tissue engineering (CFR—Code of Federal Regulations, § 184.1984). It is a plant protein obtained from corn with various industrial applications (including agriculture, cosmetics, packaging, and pharmaceuticals). Zein is classified into four types, namely α-, β-, γ- and δ-zein; α-zein accounts for almost 80% of the total amount of the natural protein, the composition of which consists mainly of glutamine, leucine, proline and alanine.

When applied as a coating solution, it gave the tablets a zero-order release. It is suitable for producing micro- and nanoparticles, micro- and nanocapsules, nanofibers and so on [51,52].

Wei et al. made core-shell microparticles to deliver curcumin (CUR) using hydrophobic zein microparticles as the core and hydrophilic cellulose nanocrystals (CNC) as the shell in the optimal ratio of 2:1. CNC adsorbed onto the surface of the zein microparticles to form the core-shell microparticles through electrostatic attraction, hydrophobic interaction and hydrogen bonding. Furthermore, the CNC allowed the formation of a compact shell that restricted the access of proteases and bile salts to the core of the microparticles, effectively reducing the release of CUR. Therefore, the use of hydrophilic nanoparticles to stabilize hydrophobic microparticles through interparticle interactions proved useful for developing new core-shell microparticles for applications in functional foods [53].

2.4. Pectins

Pectin (E440) (Figure 4) is widely used as a gelling and stabilizing agent in a variety of food products and finds increasing use in biomedical applications for its high safety, biocompatibility, and biodegradability. Chemically speaking, pectins are heterogeneous biological polymers consisting of covalently bound galacturonate molecules [27,54,55]. The exact structure is still under study due to its high variability depending on the plant source. However, the main polysaccharide components with a clearly determined chemical structure were isolated: homogalacturonan (65%), ramnogalacturonans I (20–35%) and II, replaced galacturonans, xylogalacturonan, and apiogalacturonan.

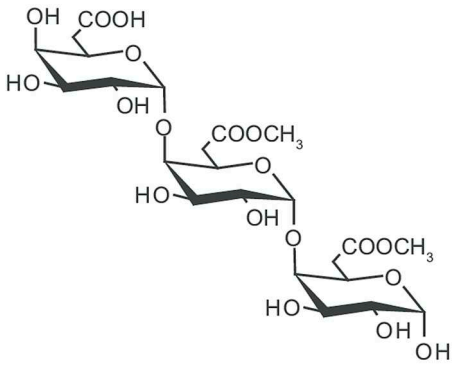

Figure 4. General structure of pectin.

More properly, the term pectin refers to a family of complex polysaccharides that are found in the cell walls of all terrestrial plants and sea grasses. Their main biological role is to provide the mechanical strength of plant parts, maintain the aqueous phase within cells through water absorption and protect cells from various environmental factors [55,56].

Lee et al. produced hydrogel microspheres as colon-targeted quercetin (QUE) delivery systems based on de-esterified pectin and oligochitosan. The systems have been preprinted with different weight ratios of pectin and oligochitosan with the ionotropic gelation (Ca^{2+}) method. The system presented the formation of a polyelectrolyte complex involving the deprotonated carboxyl groups of pectin and the protonated amine groups of oligochitosan. Cumulative release of QUE after exposure to SGF and SIF was less than 1%. Exposure to simulated colonic fluid (SCF) for 12 h showed QUE pectinase-mediated release between 65.37 and 99.54% (dependent on pectin content) [57].

2.5. Inulins

Another polysaccharide used in the preparation of colon-targeted DDS is **inulin** (Commission Regulation (EU) 2015/2314 of 7 December 2015). It is a heterogeneous natural polymer that is found in a variety of regularly consumed vegetables, fruits and cereals. Chicory root and dahlia tubers are among the most common sources, but biotechnological inulin has also been produced more recently. Inulins are mainly linear polymers consisting of 60 fructose units joined by a β(2→1) glycosidic bond (fructans) and usually ending with a glucose molecule (Figure 5).

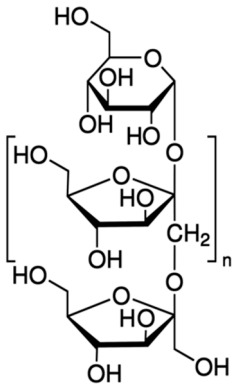

Figure 5. General structure of inulins.

The enzymes inulinase and inulin lyase, produced by the colon microbiota, are able to degrade inulin in the glucose and fructose components. Its degree of fermentation, however, depends largely on the length of the chain: long-chain inulin takes longer and degrades only in the final sections of the colon. As a prebiotic, inulin is also able to restore colon microbial balance by promoting the proliferation of commensal bacteria by inhibiting the growth of other harmful microbes [58].

Wang et al. developed micelles based on amphiphilic inulin-lipoic acid (IN-LA) conjugate (esterification) for the delivery of tanshinone IIA (TAN) for the treatment of colorectal cancer (CRC). The prepared micelles were stabilized by core cross-linking through the thiol-disulfide exchange reaction between the LA rings of the conjugate. Due to this bond (disulfide), micelles were stable in extracellular conditions, but rapidly destabilized in reductive environments typical of cancer cells due to high levels of GSH that allowed selective cargo release [59].

2.6. Shellac Gum

Shellac (E904) is another example of food-grade polymer of interest for colon targeting. It is a natural pH-sensitive amphiphilic polymer derived from a resinous substance excreted by an insect, Laccifer lacca (India, Burma, Thailand, and southern China). Shellac consists

mainly of polyester oxides with the presence of unesterified carboxylic groups with cyclic terpene acids that give it weak acidity (pKa around 6) and thus solubility in alkaline solutions (Figure 6). In the past it has been used as a natural dye in architecture, silk and leather. Its properties have attracted enormous interest in the food and pharmaceutical industries as a carrier of nutrients, foaming agents, food gelling and emulsifiers, pre- and probiotics, bioactive agents and active ingredients [60,61].

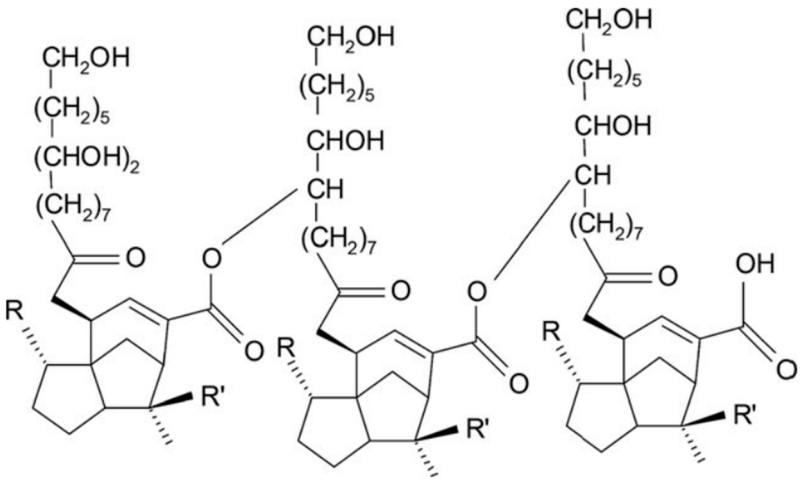

Figure 6. Chemical structure of shellac.

Wang et al. prepared colon-specific sustained-release ferulic acid (FA) shellac nanofibers by coaxial electrospinning. The in vitro dissolution test demonstrated minimal FA release at pH 2.0 and sustained release in a neutral medium. The latter occurred through an erosion mechanism, in which fibers were gradually converted into nanoparticles as FA was released and finally dissolved [62].

2.7. Eudraguard® Copolymers

The **Eudraguard®** family is a group of polymers of more recent application in the production of enteric nutraceutical formulations [63]. They are methacrylic derivatives that have arisen for the functional coating of non-chewable tablets and capsules in nutraceutical applications [40]. In a sense, they represent the food-grade equivalent of the well-known Eudragit® family of copolymers [64], which is widely known in the pharmaceutical industry to produce gastro-soluble and gastro-resistant coatings of oral solid dosage forms.

Among the members family, Eudraguard® Biotic (E1207) (EUGB) and Control (E1206) (EUGC) (Figure 7) are of great interest for the development of colon-targeted systems [41,65,66].

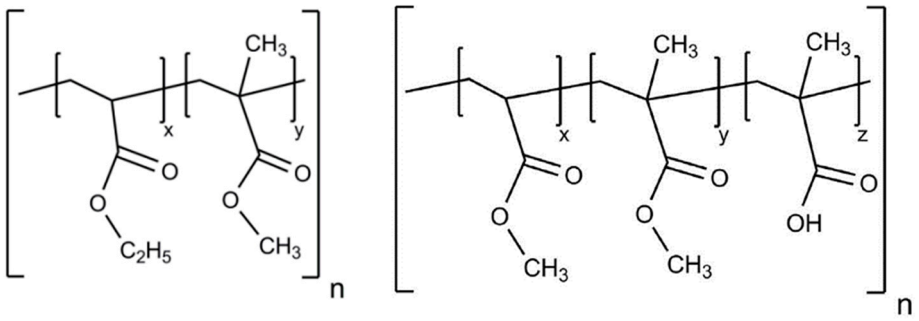

Figure 7. Schematic structure of Eudraguard® Control (**left**) and Biotic (**right**).

2.8. Natural Gums

Natural gums are widely used in foods and pharmaceuticals as viscosifying agents at low concentrations. They are hydrophobic compounds obtained mainly from plant or microbial sources. They exhibit high structural heterogeneity, so molecules have significant differences in their properties, including linear chain length, branching characteristics and molecular weight, etc. [67–71].

Gellan gum (E418) is a water-soluble polysaccharide synthesized by Sphingomonas elodea; in fact, it belongs to the sphingan family and has been widely used as a stabilizer, thickener, viscosifier, or gelling agent, but its nature allows us to explore other stimulant applications.

It was originally considered an optimal substrate for the cultivation of thermophilic microorganisms because of its heat resistance. As knowledge about its biological, chemical and physical behavior has progressed, gellan gum has attracted increasing interest in nanomedicine and tissue engineering (e.g., to produce acid- and heat-resistant biomaterials). Chemically, it is a linear anionic polysaccharide identifiable by a typical tetrameric repetitive sequence consisting of [D-Glc(β1→4)D-GlcA(β1→4)D-Glc(β1→4)L-Rha(α1→3)]n (Figure 8). The natural form of this polymer has an L-glyceryl substituent on the third carbon of the 3-linked D-Glc residue and, in some repeated units, an acetyl group on the anomeric carbon of the same residue. By heat treatment with alkali, these residues are removed and the commercial form is obtained [68,70,71].

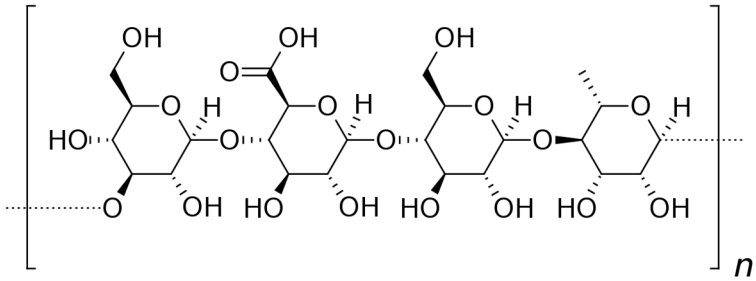

Figure 8. Structure of gellan gum.

Bhosale et al. developed a pH-sensitive drug delivery system using gellan gum conjugated to polymethyl methacrylate (PMMA-g-GG) by a radical process. The system loaded with metformin hydrochloride showed pH-sensitive and prolonged drug release over a 12 h period; the release profile followed the Peppas model [72].

Another interesting example of natural gum used in the production of modified release systems is ***almond gum*** (CFR, § 182.20). This exuded gum is obtained from wild almond trees (Amygdalus scoparia Spach.), which grow naturally in Iran and some Middle Eastern countries. Its main fraction is an anionic arabinogalactan polysaccharide (Figure 9). It exhibits different functional and biological properties depending on its molecular weight, protein content and solubility [73–76].

Salehi et al. prepared almond gum (AG) and sodium caseinate (CAS) complexes as carriers for propolis [41]. Different percentages (10 to 50 wt%) of an alcoholic propolis extract were encapsulated in the two carriers at pH 4.6 (complex coacervates) or pH 7 (soluble complexes). The antioxidant activity and %EE of the complexed coacervates were higher than those of the soluble complexes. Probably, at a pH lower than the isoelectric point of CAS (pH = 4.6), a better interaction between negatively charged AG and positively charged CAS occurs and the complex coacervates are formed. In the complexes at pH = 7, both CAS and AG have a negative charge leading to a slight electrostatic interaction between them.

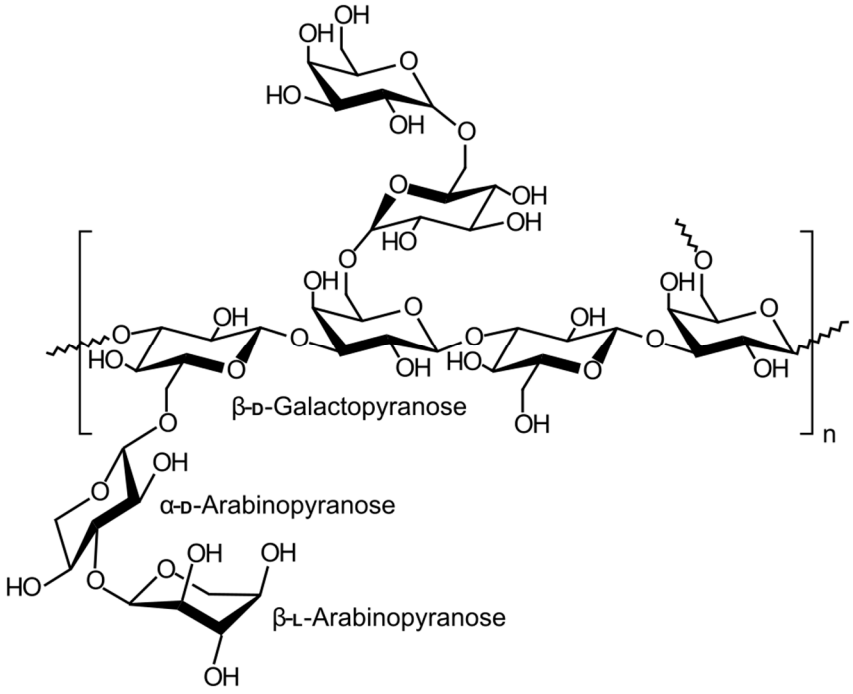

Figure 9. Structure of arabinogalactan.

The release of total polyphenol content (TPC) of propolis in different food simulants showed, after 1 h, an increasing release rate (%R) of TPC from water (%R = 60%), to 10% ethanol (%R = 68%), to 50% ethanol (%R = 85%). In the first hour of release in all food models, propolis showed a rapid release that can be explained by surface fraction of polyphenols. The maximum amount of release was obtained in 50% ethanol, due to the higher solubility of propolis in this solvent than in water. In simulated GIT environments, propolis showed a sustained release at a constant rate; the cumulative release of propolis in gastric (pH = 1.2, after 2 h) and intestinal (pH 6.8, after 8 h) environments was about 23% and 49%, respectively [77].

3. Characterization of Food-Grade Systems

Colon delivery systems for nutraceutical molecules have multiple advantages, such as the ability to overcome limitations related to the poor stability and bioavailability of active molecules. The technologies produced offer systems with sizes in the nano- and micrometric range, modify the physico-chemical properties of molecules, such as solubility and release profiles, provide protection against enzymatic degradation in the GIT tract and ensure colon-targeted delivery. Colon-target systems need to be characterized for their physico-chemical properties and then assayed by in vitro, ex vivo, and in vivo studies (Figure 10). Physico-chemical and technological characterization includes determination of mean particle size (Z-ave), polydispersion index (PdI), morphology, surface charge (Zeta potential), mucoadhesive properties, encapsulation yield, solid-state characterization (FT-IR, DSC, XRD), and drug release profile. Analysis of these parameters provides useful information to proceed to stability evaluation and in vitro/in vivo characterization. In this section we will provide a comprehensive overview of the characterization of all-food-grade systems for colon-targeted delivery.

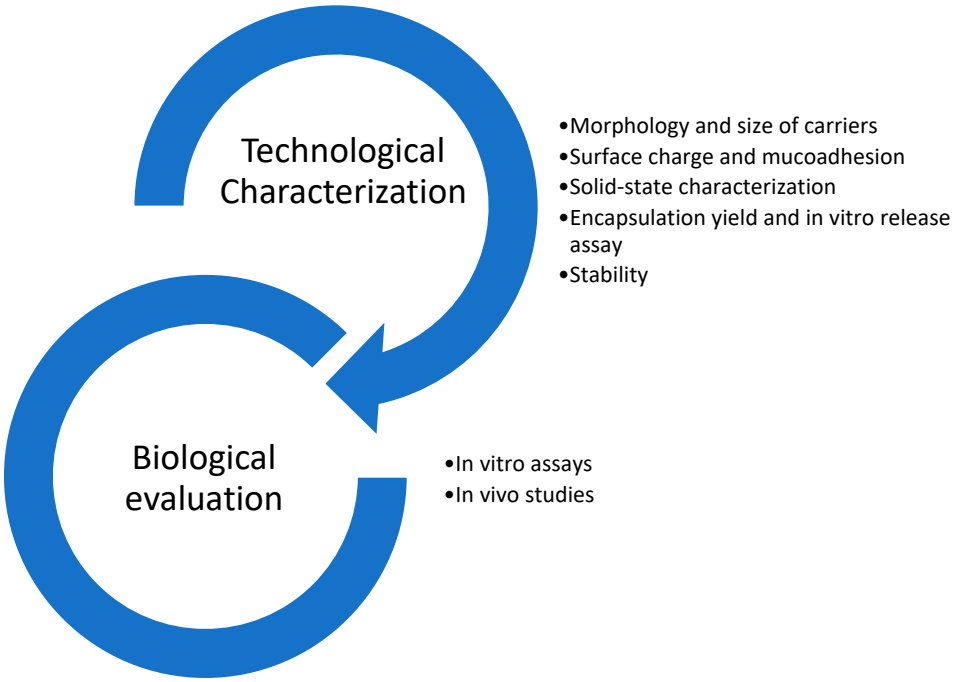

Figure 10. Characterization steps for food delivery systems.

3.1. Technological Characterization

3.1.1. Morphology and Size of Carriers

Morphology is one of the parameters that influence the efficacy and biological properties of drug delivery systems. The surface-area-volume ratio determines pharmacokinetic properties such as absorption and biodistribution, permanence in the bloodstream, and toxicity [78].

Microscopy techniques provide information on particle shape, structure, topography, and size. In the case of all-food-grade nanotechnology for colon-targeted delivery, in addition to classical uses, this method has been used for several purposes. The following are some examples.

Liu et al. prepared alginate microspheres for colon delivery of quercetin. The authors reported that water evaporation from the microspheres during the freeze-drying process caused shrinkage of the matrix resulting in surface wrinkles. In order to preserve the spherical shape of the microcarriers, inulin was added as a matrix filling material. SEM analysis showed that the addition of inulin provided effective pore filling of the alginate network, improving parameters such as gel strength and encapsulation efficiency. Moreover, comparison of morphological images of the empty and QUE-loaded systems showed that also the QUE contributed to pore filling, leading to the formation of sandy surfaces [79].

In our recent study, SEM analysis was used to evaluate the degradative processes under simulated GIT conditions of food-grade microparticles based on EUGB and EUGC and loaded with resveratrol (RSV). The morphological study showed that matrix degradation was pH- and polymer type-dependent. After 2 h of incubation in SGF, EUGB microparticles maintained unchanged and smooth surfaces, while the first signs of irregularity were detected after incubation in SIF and disaggregation after exposure to SCF, confirming a colonic-targeted release (Figure 11).

In contrast, EUGC-based samples showed irregular and porous surfaces already after incubation in SGF and SIF and only partial erosion in SCF, in agreement with the prolonged RSV release profiles. The particle size distribution of the microsystems was investigated using a multidimensional sieve shaker according to the Italian Pharmacopoeia [80].

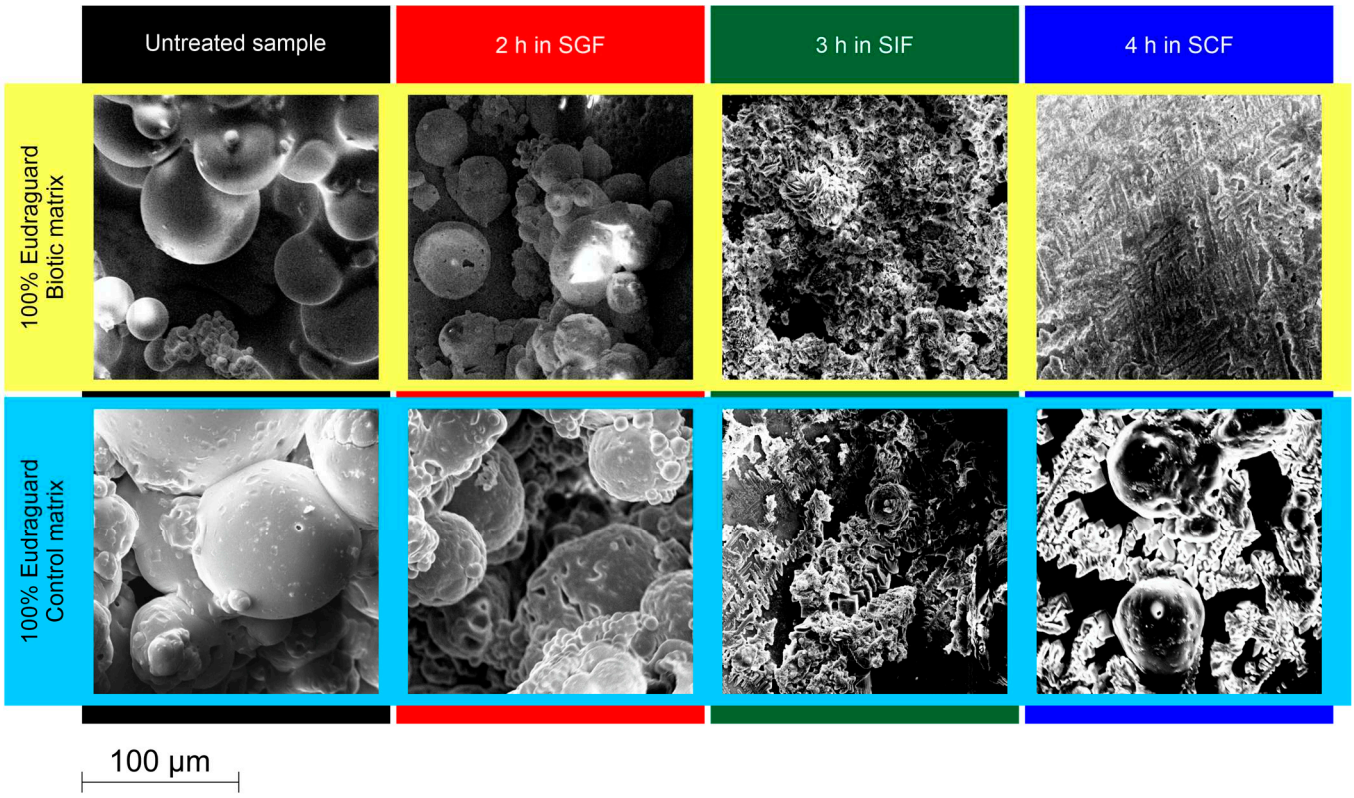

Figure 11. SEM analysis of the dissolution/erosion process of microparticles with a matrix consisting of 100% Eudraguard® Biotic and 100% Eudraguard® Control (personal data).

In a study by Sarma et al., core-shell nanoparticles for RSV delivery were prepared with a chitosan core coated with pectin. Different chitosan:pectin ratios (1:4, 1:7 and 1:15) were studied to modify the thickness of the shell. The core-shell morphology, mean core diameter, and shell thickness were investigated using three electron microscopy methods: field emission scanning electron microscopy (FE-SEM), selected area electron diffraction (FE-TEM/SAED), and high-resolution transmission electron microscopy (HR-TEM). FE-SEM images revealed spherical shape NP with a size between 23 and 32 nm. FE-TEM/SAED images were obtained to obtain information on the internal morphology and particle distribution, where FE-TEM analysis revealed the formation of monodisperse core-shell particles with a spherical core of about 13 nm and a shell with an average thickness of about 4 nm; finally, SAED imaging showed circles and bright spots that highlighted the crystalline behavior of the encapsulated RSV. HR-TEM analysis confirmed the crystalline nature and, in relation to the amount of used pectin, showed an increase in the thickness of the coating [81].

One of the limitations of electron microscopy analysis is related to sample preparation. Typically, samples for SEM analysis undergo a drying step before being coated with a metal with high electrical conductivity, while negative dyes or heavy metals are used to confer electronic transmittance in samples for TEM analysis [82].

A microscopic technique with no special sample treatments is atomic force microscopy (AFM), which is used for topographical analysis of nanomedicines. This type of morphological imaging allows to probe surfaces to obtain parameters such as roughness and other mechanical properties [83]. Recently, two nanocomplexes consisting of saponin-cholesterol were prepared and characterized by AFM. The study observed that the combination of cholesterol with the saponins escin and dioscin led to the self-assembly of nanoparticle and fibrous structures, respectively. Furthermore, it was observed that the density and roughness of the surfaces varied according to the molar ratios between the two molecules [84]. Although this technique has been introduced more recently compared with electron mi-

croscopy methods, the last ones possess advantages such as the ability to explore larger surfaces and shorter scanning times. Therefore, AFM is generally combined with SEM/TEM analysis to ensure more reliable surface characterization.

In addition to morphology, the size and PDI of nanosystems are also critically important parameters that affect properties such as release and encapsulation of the active molecule, absorption, and stability of the formulation.

Although morphological analyses also provide information regarding the average diameter of nanosystems, it must be considered that these values are determined on statistically small samples and that effective sample measurements could be modified by the procedures of sample preparation [85].

To overcome these issues and to obtain better statistics, particle average diameters are frequently measured via the dynamic light scattering (DLS) technique. DLS analysis requires a larger number of particles than microscopy techniques and describes also the interactions of the nanosystem with the solvent, providing more detailed dimensional and distributional information.

Sometimes, the correlation between measurements obtained from both DLS and electron microscopy techniques is poor, as reported in the case of the above study by Sarma et al. [80]. The authors observed that the sizes evaluated by DLS measurements were much larger (around 900 nm) than those observed with TEM analysis. These differences could be reduced when analyzing spherical particles with homogeneous polydispersion [84].

This phenomenon was confirmed in the study by Doost et al., where NPs of shellac and almond gum were prepared for quercetin delivery. The study investigated how the particle size of the nanosystems was affected by the stirring and dosing speed and the concentrations of almond gum and Tween 80, which was used as a stabilizer. Two types of electron microscopy were performed to evaluate the morphology of the samples, cryogenic scanning (cryo-SEM) and TEM. The size and particle size distribution were measured by DLS analysis. The results of the study showed that the increase in the size of NPs was correlated with a delayed nucleation rate, which was determined by both increasing the agitation speed and the higher concentration of almond gum. Conversely, smaller NPs sizes were obtained when the nucleation rate was faster, which was obtained by increasing the stirring speed and surfactant concentration. The NPs populations were homogeneous (0.252 ± 0.01), spherical in shape, and the diameters measured by the three analyses showed consistent results, indicating good agreement between the used methods [86].

3.1.2. Surface Charge and Mucoadhesion

Another critical feature of systems designed for colon targeting is the surface chemistry, which determines properties such as surface charge and mucoadhesion. These properties play an important role in the interaction of the systems with the gastrointestinal tract, as they affect mucosal penetration and tissue permeability, as well as the fate of the carriers in vivo [87]. The NPs surface could also be functionalized to ensure a site-specific response. For example, folic acid is a ligand of great interest for anticancer drug delivery, since cancer cells overexpress specific receptors for this molecule and ensure targeted action to the tumor site [88].

Carriers with mucoadhesive properties could improve interaction with the mucosal barrier and promote cellular absorption, which is an additional advantage for drug delivery in the treatment of colitis, where ulcerated walls produce a thicker mucus layer [89].

Generally, the mucus production is increased in IBD and in an inflammatory context the surface charge of the intestinal epithelium is overall cationic. With the goal of increasing mucoadhesion and epithelial retention time, many studies have focused on the production of carriers with anionic or neutral surface charges [90].

Although chitosan has frequently been used in oral delivery systems for colon-targeted delivery, the cationic mucoadhesive behavior of this polymer promotes adhesion to the upper gastrointestinal tract and impairs transport and targeting efficiency to the colon. Therefore, chitosan is often coated or combined with pH-sensitive polymers.

An example is the totally food-grade mucoadhesive system prepared by Sun et al., consisting of sodium alginate and chitosan NPs (SA-CS NPs) loaded with berberine hydrochloride to treat the colonic ulcer lesions [91]. SA-CS NPs showed a size of 257 nm, negative charge (−37.9 mV) and mucopenetrating ability. Such behavior was studied on rat colon mucus by fluorescence using Rhodamine B as a probe. For comparison, Authors used NPs made of chitosan alone (CS NPs) as a positively charged system. The small size of both NPs allowed them to pass through the pores (500 nm in size) of the mucin mesh structure, but the different surface charge affected the depth of penetration into the colonic mucosa. Indeed, positively charged NPs consisting of chitosan were retained in the superficial layer (0–200 μm) of the mucosa that, being renewed every 5 h, made the clearance of the nanocarrier easier. Conversely, the negatively charged NPs consisting of CS and alginate showed a 2.9-fold higher mucus penetration capacity, with a penetration depth over 600 μm, a positive behavior to ensure a longer permanence and accumulation of the carrier and drug in inflammation sites of the colon.

Chitosan has also been used in combination with pectin for curcumin delivery in the treatment of colon cancer. Pectin has been used both to limit the premature release of curcumin in the gastric tract but also to confer mucoadhesive properties to the nanosystems at the colonic level. Mucoadhesion was studied by dispersing the systems in solutions of mucin type III from pig stomach at different concentrations and pH (1.2, 6.8 and 7.4). The change in pH affected the surface charge of both NPs and mucin. The mucoadhesive properties of pectin under alkaline conditions were well known, but the study showed that under these pH conditions the amine groups of chitosan were also ionized, establishing stronger polyelectrolyte bonds with the mucin that had assumed a more accessible "rod-like" structure. In addition, pectin in an alkaline environment underwent swelling resulting in premature release of curcumin, but the combination with chitosan ensured the formation of more stable systems whose degradation occurred in alkaline media enriched with pectinase to provide a localized therapeutic effect. The mucoadhesive formulation obtained from the combination of the two polysaccharides proved to be an effective strategy for the delivery of curcumin targeted to the colon [92].

The surface properties expressed in the absolute value of zeta potential also determine other properties of nanosystems such as the stability of the colloidal system in the gastrointestinal tract and the redispersibility of lyophilized samples [93]. Zeta potential values indicating stability of NPs and limiting aggregation phenomena should ideally be higher than ±30 mV [94,95].

Zein has been widely applied for the development of new biomaterials such as NP. However, zein NP are prone to instability and premature release of active molecules in gastric fluids. For this reason, zein is often used combination with other hydrophilic anionic polysaccharides such as pectin and dextran sulfate [55].

In addition to its mucoadhesive properties, pectin is often used as a surface coating of nanosystems due to its stabilizing properties and low cost [56]. In study by Wang et al., core-shell NPs with a zein core and a pectin coating were prepared for delivery of the flavonoid hyperoside to the colon. The pectin coating resulted in a change in surface charge from positive (+28.9 mV) to negative values (approximately −30 mV). It was observed that the positive zeta potential of the zein NPs was neutralized as the anionic pectin was adsorbed onto the surface of the NPs. Different concentrations of pectin were studied (0.2 to 2 g/L) and it was found that when the concentration of pectin was so high as to cover the entire surface, the zeta potential maintained constant negative values. Although even the highest concentration completely coated the surface of NPs it could induce depletion flocculation and was discarded from the experiments. The pectin concentration of 1 g/L was selected because it stabilized the structure through hydrophobic effects, hydrogen bonds and electrostatic interactions and provided the highest encapsulation efficiency. In addition, the strong electrostatic repulsion between the particles induced steric stabilization that ensured excellent redispersibility of lyophilized samples and stability under simulated gastrointestinal conditions [96].

A similar study was conducted by Yuan et al., where dextran sulfate-stabilized zein NPs (ZNPs) were fabricated for curcumin delivery. By increasing the concentrations of the anionic stabilizer, the surface charge of the nanosystems gradually shifted toward negative values (Figure 12), indicating as in the previous case that the deposition of dextran sulfate on the surface of the NPs was driven by electrostatic and hydrophobic interactions. The addition of dextran sulfate not only improved the encapsulation efficiency and retention of curcumin in NPs, but also ensured increased bioaccessibility of the molecule in an in vitro model of simulated digestion. The increased bioaccessibility of curcumin could potentially promote absorption into the systemic circulation and thus improve in vivo bioavailability [60].

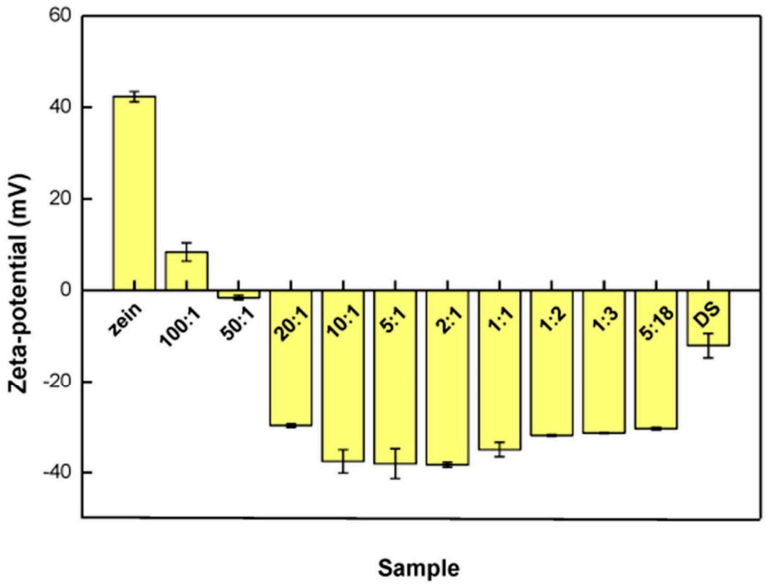

Figure 12. Zeta potential of zein NPs in the absence and presence of dextran sulphate at different mass ratios and at pH = 4.0. Adapted with permission from Ref. [60]. 2019, Elsevier B.V.

Therefore, appropriate surface properties, such as resistance to gastrointestinal digestion and mucoadhesive and mucopenetrating features, need to be imparted to the nanosystems to ensure that the carriers can be effective colon tract-specific delivery systems.

3.1.3. Encapsulation Yield and Solid-State Characterization

It is well known that bioactive constituents, including vitamins, bioactive lipids, bioactive peptides, essential oils and even probiotics, have a number of potential health benefits. These, however, are sensitive to heat and possess poor chemical stability. Several encapsulation methods have been applied to protect these constituents from thermal and chemical degradation. Encapsulates prepared by different methods and/or under different conditions have different microstructures, which in turn affect the efficiency of encapsulation, the retention of encapsulated substances, and the controlled release behavior of encapsulates differently [97].

In this context, the determination of specific parameters such as encapsulation efficiency (%EE) and drug loading (%DL) through the following Equations (1) and (2) allow the quantification of encapsulated material [98–100].

$$\%EE = \frac{(\text{Total drug added to the beads} - \text{Amount of free drug})}{\text{Total amount of drug added to the beads}} \times 100 \quad (1)$$

$$\%DL = \frac{\text{Amount of drug loaded in the beads}}{\text{Total weight of the beads}} \times 100 \quad (2)$$

During the encapsulation process, constituents reorganize into the neostructure of the system. This is dependent on the nature of the substances to be encapsulated and the encapsulants and the encapsulation process. In this sense, the assessment of any interactions between the carrier constituents and the carrier active substance and the nature of its solid state (crystalline or amorphous) within the system and the system itself are of crucial importance to the processes of development, formulation, activity, and storage. These, for example, affect not only the preparation of the system but also the possible dissolution-erosion mechanisms of the carrier, the mechanisms and profiles of release of the filler, its dissolution and thus its bioavailability and stability. For this purpose, the constituents of the system, their physical mixture(s), empty and loaded system are subjected to specific analyses, among which FT-IR, DSC and PXDR are the most common.

FT-IR analysis provides information about the chemical bonds present in the sample giving us important information about the formation of any interactions between the constituents of the system [98,101,102]. DSC allows to assess the temperatures at which characteristic endothermic and exothermic transitions occur and that are specific for a certain substance and its structure. These can indicate the melting point of the sample or more generally a state transition (e.g., a rubbery-glass transition) and its purity, and confirm any interactions between samples in mixture or neostructured in a carrier system [103–105].

PXDR analysis provides information about the structure of the solid state, allowing to observe crystalline or amorphous transitions following the formulation production process [106–109].

All these techniques synergistically allow the evaluation of the encapsulation process of the carrier substance [110]. For instance, absence of the characteristic peaks of the active substance in the spectra of the loaded system indicates its complete and uniform encapsulation in the carrier matrix.

To this end, Curcio et al. used FTIR, DSC and PXDR in the technological characterization of microparticles based on EUGB and EUGC prepared for quercetin (QUE) delivery to the colon. The study investigated different formulation approaches by mandating fixed concentration of QUE and predetermined QUE:copolymer weight ratios (1:5, 1:10 and 1:25). The system consisting only of EUGB had a %EE of 97.6%. The FT-IR spectrum of the loaded system was superimposable with that of EUGB, and the characteristic QUE peaks were not present. This confirmed the absence of degradation or alteration processes during formulation and the successful encapsulation of QUE. In addition, the absence of significant changes in the OH stretching band region (3200–3600 cm^{-1}) and the C=O stretching band region (approximately 1735 cm^{-1}) confirmed the absence of chemical interactions between the flavonoid's carbonyl and carboxyl groups and the polymer. A similar behaviour was observed for the system consisting of EUGC alone, with a %EE of 69%. The encapsulation process was also confirmed by DSC analysis. In fact, the thermogram of microparticles loaded and produced with increasing weight ratios of QUE:EUGB showed no thermal transitions corresponding to QUE. The endothermic peaks recorded around 120 °C were attributed to dehydration phenomena observed for both pure crystalline QUE and EUGB. XDR analysis also confirmed the homogeneous dispersion of polyphenol within the matrix. Furthermore, these results indicated that the encapsulated QUE was present in a disordered non-crystalline or highly microcrystalline state within the polymer network [41].

Previously, other authors have designed a NP delivery system for the encapsulation of bioactive compounds using QUE as a model. A combination of almond gum (AG) and shellac was used to prepare the system using the antisolvent method. The %EE of the NP made by the biopolymers combination without surfactant was about 78%, and no considerable improvement was observed when the concentration of QUE was increased to 0.05%. In the presence of surfactants (PS 80 or QS) and 0.01% QUE, it was 91 and 87%, respectively, which increased considerably to 99% with 0.05% QUE.

The increase in %EE with the addition of a surfactant may be related to the increased solubilization of QUE molecules due to the presence of surfactant and the formation of smaller particles leading to increased saturation solubility.

The thermogram of the charged NPs (Figure 13a) showed no endothermic peak at 320 °C (melting peak characteristic of pure, crystalline QUE) indicating that the drug was well mixed with shellac as a base material within the system and most likely QUE existed in an amorphous form as a solid solution, rather than in crystalline form. It must be emphasized that the amorphization of QUE would enhance its solubility at the gut pH conditions, and thus bioavailability. The FT-IR spectrum (Figure 13b) of charged NPs showed the characteristic peaks of the alcohol group of AG around 1000 cm^{-1} and the C-H group of shellac (2860–2930 cm^{-1}). In this spectrum, the peak intensity of pure QUE around 1500 cm^{-1} (aromatic ring) was clearly reduced indicating that an interaction between QUE and shellac molecules had most likely occurred [111].

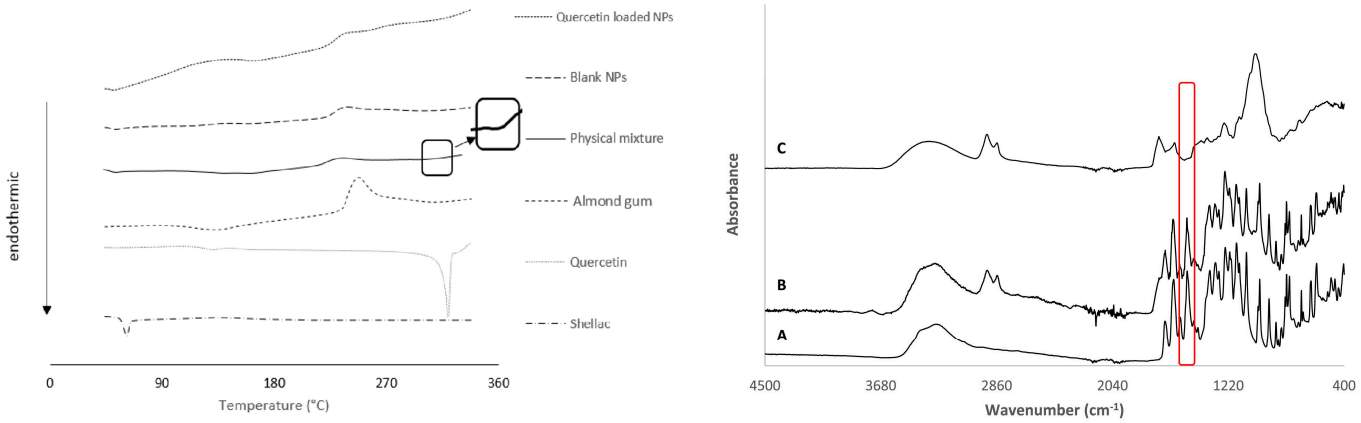

(**a**) (**b**)

Figure 13. (**a**) Comparison of DSC thermograms of pure compounds (shellac, quercetin, and almond gum) as well as their physical mixture, blank nanoparticles, and quercetin loaded nanoparticles and FTIR spectra of pure quercetin (A), physical mixture (B), and quercetin loaded NPs (C). (**b**) FTIR spectra of pure quercetin (A), physical mixture (B), and quercetin loaded NPs (C). In the red box, it is observed that the peak intensity of pure quercetin around 1500 cm^{-1}, assigned to the aromatic ring, decreased in the spectrum of quercetin-enriched NPs. This indicates that an interaction between quercetin and shellac molecules most likely occurred. Adapted with permission from Ref. [111]. 2018, Elsevier Ltd.

A study published in Food Biophysics focused on the development of a zein-sodium caseinate-xanthan gum (Z-SC-XG) nanocomplex for piperine (PIP) delivery. FT-IR spectra of the developed nanocomplex showed a broadening of the peak at 3408 cm^{-1} attributable to the hydrophilic O-H stretching of Z and a decrease in the intensity of the hydrophobic C–H stretching at 2924 cm^{-1} attributed to CS. These changes are due to the hydrophilic increase in the PIP/Z-SC-XG complex with respect to Z due to hydrophilic XG. In addition, the shift and decrease in intensity of the peaks associated with the amide bonds (amide I, II and III) of SC was detected. Similarly, a decrease in the intensity of the peak associated with the vibration of the carboxyl group of XG was observed. These changes could indicate an interaction between the amine groups of Z and SC and the carboxyl groups of XG as a whole. In addition, in PXDR analysis of PIP/Z-SC-XG, the characteristic peaks of Pip in the solid state were not detected, indicating that it was well encapsulated in the protein and polysaccharide matrix. Additionally, small peaks were detected at 9.6° and 19.8° assigned to the presence of zein in the nanocomplex structure. The much lower intensity of these peaks, compared with those observed in the diffractogram of pure sein, could be due to the changes in the organization and molecular interactions of zein in the presence of SC, XG and PIP [112].

3.1.4. In Vitro Release Testing

In the context of DDS and its corresponding food applications (dietary supplements and fortified food), in vitro release testing aims to evaluate over time the amounts of loaded substance that are released from the system under conditions simulating GIT. The extensive literature available proposes different protocols (direct beaker dissolution, dissolver dissolution, dialysis method, etc.) for colon-targeted DDS [65,113–115]. Therefore, in order to properly compare release profiles different variables must be considered including, intrinsic properties of the system (shape, size, rheology/viscosity, nature of components and their interactions, if any, production procedures, %EE and/or %DL and release mechanism, etc.), number and type of simulated environments (mouth, stomach, intestine, colon and any other specific sections) and their specific reference parameters (simulated environment in empty or fed conditions, pH, travel time, volumes and fluid composition, thus presence or absence of specific enzymes, surfactants, salts, etc.) [7,46,104,116–120]. Added to this is the common research effort to develop in vitro dissolution/release equipment/protocols with increasing significance and predictivity of the in vivo process [121–123]. During the test, aliquots are taken and appropriately treated and are subjected to quantitative analysis of the released active substance (e.g., HPLC and UV). From the data obtained, profiles and release kinetics are derived. All these data allow us to assess the proportion of the active substance available for uptake, i.e., bioavailable, or in situ action. Referring to recent scientific literature, we propose an overview of this stage of the characterization of total food-grade systems for targeted delivery to the colon.

Curcio et al., studying polymeric systems based on EUGB and EUGC for colon-targeted delivery of RSV, carried out an in vitro release test according to the pH-varying model provided by the Eur. Pharm. X Edn. (Method A, Apparatus 2, Delayed-release solid dosage forms) with some minor modifications. Briefly, 750 mL of a 0.1 N HCl solution to simulate the gastric environment at pH 1.2 (SGF) and the sample to be analyzed were placed in the beaker of the paddle dissolver (thermostated to 37 ± 0.5 °C). After 2 h to simulate the intestinal environment, the pH was raised to 6.8 (SIF) by adding 250 mL of a 0.20 M Na_3PO_4 solution. Finally, the colon environment was simulated after 8 h by bringing the pH to 7.4 (SCF) with a few drops of a 3N solution of NaOH. The test had a total duration of 24 h. Aliquots of the medium replaced with equal volume of specific fresh buffer were taken at predetermined intervals. By UV analysis, the corresponding release rates were derived. All systems prepared with EUGB exhibited low releases under simulated gastric conditions (less than 30%) except for the one with the RSV:EUGB weight ratio of 1:5 in which 40% release was exceeded. This is probably due to the presence of unencapsulated RSV as confirmed by the low value of %EE = 75.2% and FTIR and DSC analysis. In addition, it was shown that the release rate gradually increased in SIF to reach the plateau in simulated colonic environment. The test showed that the minimum RSV:EUGB weight ratio required to control RSV release was 1:10; whereas systems with weight ratios of 1:20 and 1:50 had nearly overlapping release profiles. Systems formed from EUGC alone had low sustained RSV release. Mixed matrices allowed the release plateau to shift (about 80%) in the interval 4–8 h after the start of the test (SIF-SCF) with release rates in the gastric environment varying from 20 to 60% [65].

The in vitro release of RSV from pectin-zinc-chitosan nanoparticles (10:1:3) with or without polyethylene glycol (PEG) prepared (%EE = 63% with PEG) by Andishmand et al. was studied by dialysis technique. The optimized system had a particle size of 83 ± 4 nm and a Zeta potential of 25 ± 1 mV in the presence of PEG with an encapsulation efficiency of about 63%. To simulate the gastric environment without enzymes, 1 mL of the system was placed in the dialysis tube and suspended in 20 mL of HCl (0.1 M)-ethanol (in an 80:20 ratio) (pH = 1.2). Next, it was it suspended in 20 mL of phosphate-ethanol buffer (in an 80:20 ratio) (pH = 6.8) to simulate the condition of the small intestine. Finally, the colonic environment was simulated by raising the pH to 7.4 in the presence and absence of 0.6 mg/mL pectinase enzyme. The test was conducted under agitation in an incubator (50 rpm, 37 °C). The study, in addition, analyzed the release behavior in the pH of grape juice (for potential

use in fortified food production) by incubating 1 mL of the system inside a dialysis tube in 20 mL of acetate buffer. The pH was adjusted to 3.5 and 4.5 with 0.1 M acetic acid for one month at 4 °C. In vitro release studies in different simulated gastrointestinal media concluded that 49% and 60% of RSV was released into the simulated colonic environment by the nanoparticles with and without PEG, respectively. Finally, under the conditions simulating grape juice, the-PEG system recorded a higher cumulative release of RSV than the PEG-free form. Therefore, it is more likely that the role of NH_3^+ groups in swelling at low pH was not as impressive as that of COO^- groups at pH 6.8 and 7.4 [124].

In another study published in Chinese Medicine, microparticles (Shellac@Cur/MPs) were prepared with the core (zein)-shell (shellac) structure based on coaxial electrospray technology. The particles had an average hydrodynamic size of 2.8 μm, a zeta potential of −25.3 mV and a high encapsulation efficiency over 95%. Three types of release media with different pH values were applied to simulate the digestive tract environments, namely artificial colonic fluid (pH 7.8), artificial intestinal fluid (pH 6.8) and SGF (pH 1.2). Both Cur/zein MPs and Shellac@Cur/zein MPs suspended in PBS (equal to 400 μg of Cur) were introduced into a dialysis tube. The closed tube was placed in a centrifuge tube with 40 mL of the release medium at 150 rpm and 37 °C for 16 days. At predetermined intervals, an aliquot was taken for HPLC analysis. Both Cur/zein MPs and Shellac@Cur/zein MPs showed very slow-release profiles at pH 1.2, indicating that both systems could prevent burst release of the filler into the acidic stomach microenvironment due to the hydrophobicity of the zein and shellac materials. The intestinal release of CUR from Cur/zein MPs after 11 days had reached 45%. In the presence of shellac, the release was more sustained. CUR release from Shellac@Cur/zein MPs was disruptive at pH 7.8, indicating the pH sensitivity of shellac material [124].

In a study published in Gels, a core-shell bioactive release system was prepared using natural food-grade materials. The beads were fabricated by mixing WPI (whey protein isolate) emulsion with pectin using the ionotropic gelling method. The incorporation of high pectin content into the system affected its texture, network structure and thermodynamics. Since the degree of swelling is a crucial factor in the release of quercetin from these systems, the swelling properties of all beads were measured in distilled water after immersion at 25 °C for 6 h. Beads containing 40% pectin showed the highest swelling ratio after 6 h (48.5%) indicating a porous structure. In contrast, those with 20% had markedly decreased after 3 h, probably indicating the loss of structural integrity following the absorption of water molecules and subsequent dilution of the polymer. The in vitro release test found a maximum release of 10% quercetin for the beads with 20% pectin in SIF. This showed high stability of the systems in SGF and SIF indirectly indicating the potential for use as colon-targeted nutraceutical delivery systems [125].

Liu, S. et al. developed hollow/QUE-filled microspheres of alginate (AL-E/Q), alginate/inulin (ALIN-E/Q), and alginate/inulin/chitosan (ALINCH-E/Q), with particle sizes ranging from 25.1 ± 1.8 to 79.4 ± 4.5 μm.

The presence of inulin allowed the enlarged pores of the alginate lattice to be occluded in an alkaline environment constituting an additional factor controlling release. In vitro gastrointestinal digestion was performed with a protocol (INFOGEST) simulating the progression in saliva (SSF), gastric fluid (SGF, pH = 3) and intestinal fluid (SIF, pH = 7).

The combination of inulin as the pore-filling material of the alginate network and chitosan as the coating material in loaded ALINCH-Q (%EE = 53.2 ± 1.2%) outperformed the other formulations with a QUE retention rate of 80.3 ± 4.4% after in vitro gastrointestinal digestive treatment. Therefore, ALINCH-Q was subjected to colonic fermentation (Figure 14) using pig fecal material as the source of microbiota. Fecal inoculum was prepared by homogenizing 20 g of freshly collected porcine feces (from four healthy females) in 80 mL of sterilized 0.1 M phosphate buffer (pH = 7.0) and filtered through a sterile muslin cloth. Fermentation was conducted by adding 100 mg of microspheres in 5 mL of sterilized basic culture medium to which 5 mL of fecal inoculum was added, and the mixture was washed with nitrogen, vortexed and incubated in anaerobiosis under positive nitrogen

pressure for 24 h. Free QUE was gradually metabolized by the porcine fecal microbiome, disappearing over the 24 h of fermentation, but encapsulated QUE (ALINCH-Q) delayed metabolism. In fact, at time zero, the free form had the highest level (0.39 mg/mL), and then gradually decreased with time, while for the (ALINCH-Q) system, a minimum amount of encapsulated quercetin was detected and then reached 0.33 mg/mL concentration in the fermentation fluid at 3 h. The level of quercetin in both cases decreased substantially within 6 h, and by 12 h most was degraded to phenolic metabolites by the action of the porcine microbiome.

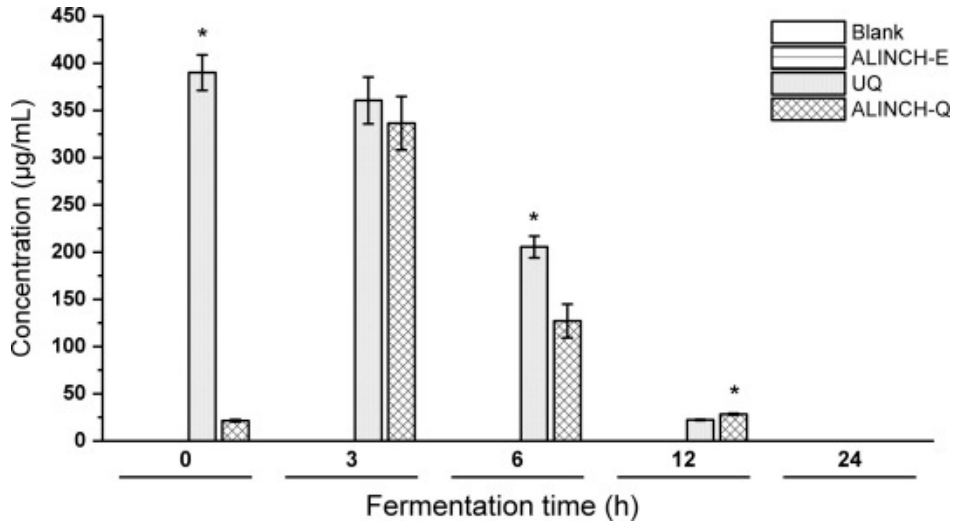

Figure 14. Quercetin degradation during 24 h of in vitro colonic fermentation. Blank: no substrate addition (10 mL fecal inoculum), ALINCH-E: empty microspheres (100 mg/10 mL fecal inoculum), UQ: unencapsulated quercetin (5.46 mg quercetin in 10 mL fecal inoculum, equivalent to the amount encapsulated in 100 mg ALINCH-Q), ALINCH-Q: quercetin loaded microspheres (100 mg containing 5.46 mg encapsulated quercetin/10 mL fecal inoculum). Quercetin in fermentation fluid was extracted into 80% methanol and was determined by HPLC. Statistical analysis was done using One-way ANOVA. * Represents significant difference compared to the other treatment group within each time point at $p < 0.05$. Note that there is no detectable quercetin in both Blank and ALINCH-E. Adapted with permission from Ref. [79]. 2022, Elsevier Ltd. All rights reserved.

Since chitosan is poorly fermentable by intestinal bacteria, it would appear that the release of quercetin is mainly due to ionization of the carboxyl groups of alginate at neutral pH (enlargement of the hydrogel network) and its degradation by excreted microbial polysaccharide hydrolases.

From the results obtained, ALINCH-Q microspheres have been proposed as a valid system for the sustained release of QUE by prolonging its retention time during colonic fermentation [79].

A more recent study published proposed an interesting site-specific delivery system of nutraceuticals for ulcerative colitis (UC). The natural anti-inflammatory products berberine (BBR) and epigallocatechin gallate (EGCG) were assembled (BBR/MPN NPs) and encapsulated in yeast microcapsules (YM), generating the BBR/MPN@YM system (%EE = 62.45 ± 1.16% for BBR and %EE = 95.27 ± 0.33% for EGCG).

The system was designed for site-specific delivery to inflammation-prone areas of the colon for the treatment of ulcerative colitis. Indeed, due to the rigid structure of β-glucan on the yeast microcapsules, decomposition of the system by gastric acid and pepsin could be reduced to a certain extent. Upon reaching the colon, the system could be phagocytosed by M cells, transported into the payer's patch and internalized into macrophages. Then, the degradation of β-glucan and nanoparticle structure could allow the release of BBR and EGCG by transforming M1 macrophages into anti-inflammatory M2

macrophages, thus exerting specific anti-inflammatory effects. Therefore, the release rates of BBR/MPN NPs and BBR/MPN@YM were evaluated in environments simulating the normal gastrointestinal tract (GIT) and in the presence of IBD (GIT-IBD).

The cumulative release of BBR from BBR/MPN@YM in the GIT and GIT-IBD showed almost the same trend in the first 6 h. After which, due to the acidic conditions of the colonic segment in the IBD model (pH = 3.5), which was different from that of the normal colon (pH 7.4), more BBR was released in GIT-IBD indicating that the prepared system allowed for a greater and faster release of the nutraceuticals at the colitis site [126].

3.1.5. Stability

Due to various environmental factors, including temperature, humidity, light, pH, etc., dietary supplements and pharmaceutical products can undergo degradation processes (chemical, physical, and microbiological) that affect their efficacy and/or safety. In general, we can define stability as the ability of a product to maintain its chemical, physical, and microbiological properties during its storage and use period. Specifically, chemical stability refers to the ability to maintain chemical identity and bioactive properties, physical stability to the retention of shape, color, odor, taste, and other physical characteristics, mind microbiological stability to retain sterility (or a low level of microorganisms) [127,128]. EMA (European Medicines Agency) and EFSA (European Food Safety Authority) for EU, FDA (Food and Drug Administration) for the USA, and PMDA (Pharmaceuticals and Medical Devices Agency) for Japan are concerned with the regulation and safety of food and pharmaceutical products. The International Council for Harmonization of Technical Requirements for Pharmaceuticals for Human Use (ICH), along with the World Health Organization (WHO), has provided a set of guidelines (ICH Q1A-E, Q3A-B, Q5C, Q6A-B) intended to unify the standards for the European Union, Japan, and the United States to facilitate the mutual acceptance of stability data that are sufficient for registration by the regulatory authorities in these jurisdictions [129]. Finally, with particular emphasis on microbiological stability, the International Organization for Standardization (ISO) with its ISO 14,698 standard outlined the importance of microbiological risk assessment in airy environments and on products. In summary, stability assessment aims to investigate the maintenance of parameters (chemical, physical and microbiological) of the system over time. Therefore, the stability of active ingredients, nutraceuticals, pre- and probiotics, and other bioactive substances can be compromised by environmental factors for which encapsulation in appropriate systems in addition to enabling targeted delivery to the target site allow for improved stability [130–132]. Systems produced in this way are also subject to degraded phenomena, so careful monitoring of specific parameters over time is necessary. For example, in assessing the physical stability of micro- and nano-emulsions, colloidal systems, and solid-liquid dispersions of microsystems, size, PDI, and PZ are of relevant importance. In fact, their monitoring makes it possible to assess the occurrence of phenomena such as sedimentation, creaming, rupture, flocculation, and so on that compromise the stability of the preparation. To avoid the occurrence of these phenomena and thus increase stability, it is possible, for example, to minimize and homogenize the particle (or droplet) size, increase the viscosity of the dispersing medium, increase the stability at the droplet interface, give the system PZ values of $\pm$30 mV to ensure proper electrostatic repulsion, the inclusion of the dispersing put of inert polymers with high steric bulk, and so on [133–136]. Therefore, as stability assessment is particularly important for food and pharmaceutical products, as their efficacy and safety can be compromised by chemical, physical, and microbiological processes, we propose some examples of stability assessment of food-grade polymer-based colonic-targeted systems found in the literature.

Kong et al. proposed an interesting stability study of chlorophyll encapsulated in shellac nanoparticles immobilized in an agarose gel and encapsulated in calcite crystals. The chlorophyll-loaded nanoparticles (83 and of 108 nm) were tested for 56 days. Both samples showed 80% chlorophyll retention after 28 days at 4 °C and subsequent 28 days at room temperature. The pure chlorophyll dispersion, prepared as a reference following the

same procedure, exhibited a gradual shift of the absorption peak from 670 nm to 690 nm over time. This was associated with a color transition from green to yellow indicating chlorophyll degradation. These phenomena were absent in the analysis of encapsulated chlorophyll. In fact, the absorption peak at 670 nm decreased only slightly after 56 days and the dispersions showed a constant green color. However, the authors point out the possibility of degradative phenomena as a result of the slow diffusion of water and oxygen through the matrix. To demonstrate the enhanced stability of the crystal-encapsulated compounds, they and the nanoparticles alone were tested at room temperature under strong simulated solar irradiation. Chlorophyll retention was monitored by measuring its fluorescent intensity, since chlorophyll catabolites obtained from the photodegradation process are not fluorescent. After 109 h, encapsulated in the nanoparticles, less than 10% of the chlorophyll remained, as light had greatly accelerated its degradation. In contrast, 80% of the chlorophyll encapsulated in the crystalline composites did not degrade. Therefore, calcite crystals, with a dense and highly ordered structure, could provide an excellent barrier to protect chlorophyll from hostile environments, resulting in increased stability [137].

Other researchers focused on the impact of nanoencapsulation in a xanthan gum-shellac matrix on the thermal stability of cinnamon extract. The test was conducted in a water bath at a temperature of 90 °C. Samples were collected after 20 min of heat treatment. The total phenolic content and antioxidant activity (phosphomolybdenum and FRAP methods) of the samples before and after heat treatment were analyzed. After heat treatment, the polyphenol retention of the free cinnamon extract was about 84%, while that of the nano-encapsulated form was 94%. However, nanoencapsulation was not able to perfectly prevent the thermal degradation of cinnamon polyphenols, probably due to a proportion of unencapsulated polyphenols, as confirmed by the encapsulation efficiency of 30%. In fact, the nano-encapsulated cinnamon extract had an antioxidant activity of 88% versus 85% of the free extract [138].

A study published in Food Chemistry addresses the stability of simulated GIT, pH and ion (NaCl) environments of nanoparticles based on a ternary zein/tea polyphenol/pectin complex loaded with HYP (Z/TP/P-HYP). The potential application of Z/TP/P-HYP as a vehicle for oral administration of HYP was studied by evaluating its stability under conditions simulating gastrointestinal conditions. Specifically, the conditions of the fasting stomach (pH 2.0 and presence of pepsine), fed stomach (pH 4.0 in presence of pepsin) and intestine (pH 7.4 in presence of pancreatin) were simulated. After 2 h under gastric conditions at pH 2.0, the Z-HYP nanoparticles aggregated (probably due to the presence of zein) to form particles larger than 300 nm (PDI > 0.3). They showed increased stability after 2 h of incubation under pH 4.0 conditions. Even after 4 h of incubation under intestinal conditions, Z-HYP exhibited aggregation (probably due to reduced charge). The presence of pectin and TP-pectin (providing a steric stabilizing effect) is the probable cause of the improved resistance of Z/P-HYP and Z/TP/P-HYP to pancreatin digestion. These data allow us to affirm the high application potential in colon-targeting. The ionic stability of the systems was investigated in the pH range of 2.0–8.0. The samples, after dilution, were brought to the desired pH using a 1.0 mol/L hydrochloric acid solution or a 1.0 mol/L sodium hydroxide solution. At pH 6.0, a significant increase in Z-HYP particles was observed with subsequent aggregation probably due to the presence of zein (isoelectric point at pH 6.2). In fact, as pH increased, the zeta potential of Z-HYP changed from positive to negative and then became neutral at pH 6.0. Z/P-HYP and Z/TP/P-HYP showed no significant size and zeta potential changes and better stability against aggregation over the pH range examined. This suggested that TP did not contribute significantly to surface charge and that pectin may play a dominant role in the electrical characteristics of Z/TP/P-HYP. Finally, ionic stability was evaluated by mixing NaCl solutions at the predetermined concentrations of 0, 100, 200, 300, 400 and 500 mM to the diluted samples and subsequent overnight incubation at 25 °C. Z-HYP already at the concentration of 100 mM showed an increase in particle size with aggregation/sedimentation. This phenomenon may be due to the salt counterions neutralizing the charge of Z-HYP, weakening the electrostatic

repulsion between the nanoparticles. The presence of pectin and TP significantly improved the ionic stability of Z/P-HYP and Z/TP/P-HYP. Particle size (Z/TP/P-HYP < Z/P-HYP, probably due to the lattice of TP) was found to be proportional to NaCl concentration. In contrast, the surface charge was found to be inversely proportional. In the absence of ions in solution, electrostatic repulsion was sufficient to overcome hydrophobic and Van der Waals interactions between the particles to prevent aggregation.

The study evaluated and compared (SC50 values) the DPPH and ABTS radical scavenging abilities of free HYP. The ability of Z/P-HYP and Z/TP/P-HYP to scavenge the DPPH radical was 3.3- and 4.5-fold stronger than that of free HYP, respectively. Higher values (1.9- and 2.7-fold, respectively) than that of free HYP were also shown for the scavenging activity of the ABTS radical. Probably the nanoscale coupled with the better dispersibility of the encapsulated HYP favored the reaction with free radicals in the aqueous phase [139].

The Turbiscan® analysis conducted by Bonaccorso et al. provided information on the physical stability of the colloidal suspensions of the systems they prepared. In order to improve the viability of probiotic bacteria delivered with fruit juice, encapsulation of *Lacticaseibacillus rhamnosus* strain GG in alginate systems (optimized microspheres with a diameter of about 1000 nm) was proposed.

The test recorded, after 7 days at 25 °C, for both the empty and loaded systems higher TSI (Turbiscan® stability index) values (Figure 15a) than for the fruit juice alone showing that the alginate systems accelerated pulp sedimentation. Non-significant instability phenomena (ΔBS > 10%, Figure 15b–d) due to the reversible migration of particles in both the lower and upper part of the cuvette were also evidenced [140].

3.2. Biological Evaluation

3.2.1. In Vitro Assays

In preclinical research, in vitro models play a crucial role in establishing the potential therapeutic effects before moving to in vivo experimentation. In addition, conducting extensive in vitro studies is of great importance to ensure successful formulation with less demanding techniques than animal experiment, both on the economic and ethical fronts. Culture techniques are used to study the cytotoxicity, permeability, and targeting efficacy of formulated systems [141]. Some examples of the reviewed articles are discussed below.

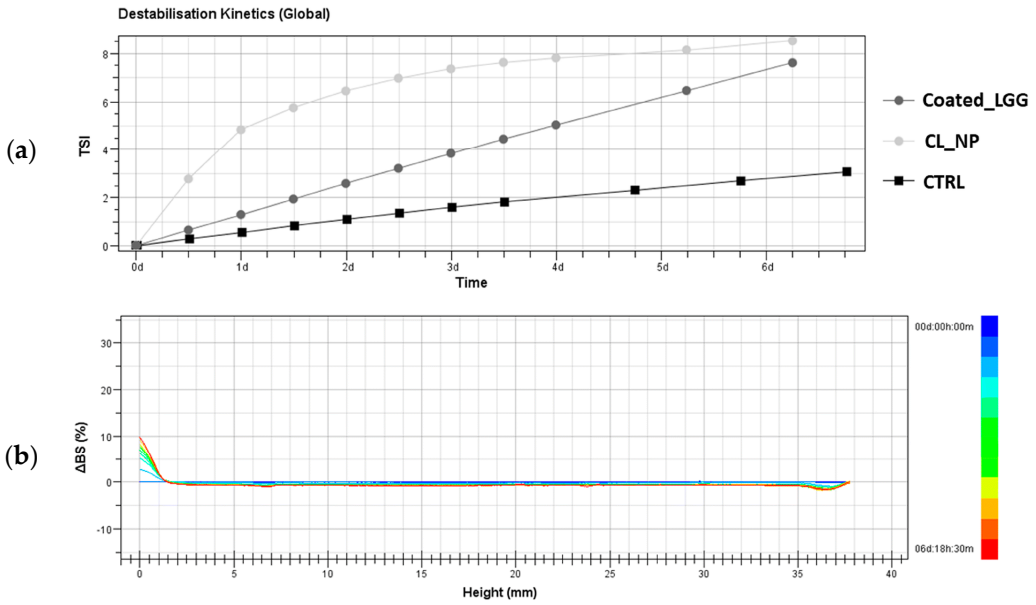

Figure 15. *Cont.*

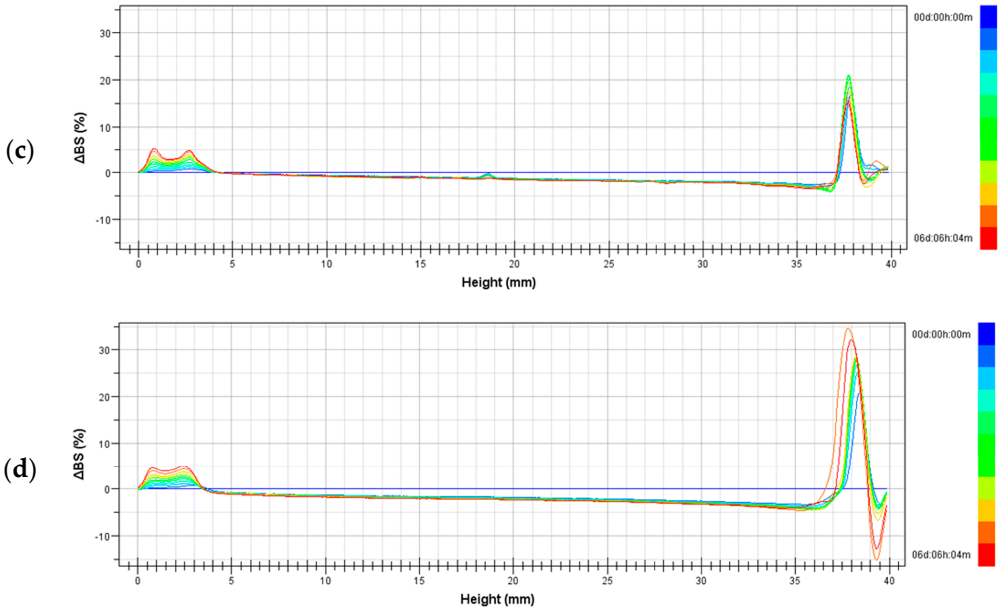

Figure 15. Destabilization kinetics expressed by Turbiscan Stability Index (TSI) of orange fruit juice (CTRL), empty cluster of nanoparticles (CL_NP), and coated Lacticaseibacillus rhamnosus GG (Coated_LGG) stored 7 days at 25 °C (**a**) and backscattering profiles (ΔBS) of orange fruit juice (CTRL) (**b**), empty cluster of nanoparticles (CL_NP) (**c**), and coated Lacticaseibacillus rhamnosus GG (Coated_LGG) (**d**) stored in Turbiscan® at 25 °C for 1 week. Adapted with permission from Ref. [140], 2021, The Author(s).

To alleviate the inflammatory disorders of ulcerative colitis, totally food-grade silk sericin (SS) nanocarriers loaded with proanthocyanidins (PAC), natural polyphenols with free radical scavenger activity, were fabricated. The in vitro study showed that the antioxidant activity of the nanosystems, in addition to being exerted by the polyphenols, was also exerted by the silk sericin matrix. The ferric reducing antioxidant potential (FRAP) assay showed that the combination of the two components synergized the antioxidant properties of the individual compounds in a concentration-dependent manner. Irritation of nanocarriers on mucous membranes was evaluated on a chorioallantoic membrane (CAM), which showed the absence of signs of irritation such as hyperemia, hemorrhage, and blood vessel coagulation even at the highest concentrations tested (Figure 16).

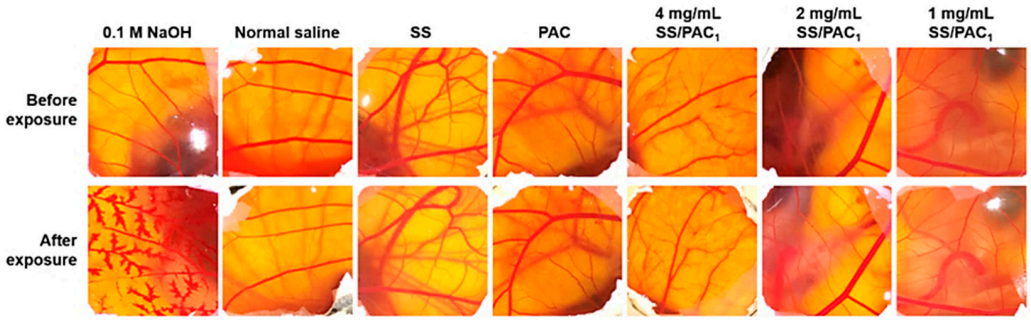

Figure 16. Photographs of CAM before and after exposure to SS, PAC, and SS/PAC1. adapted with permission from Ref. [142]. 2022, Elsevier B.V.

Hemocompatibility was studied by observing hemolysis induced by samples incubated with fresh blood. Encapsulation of proanthocyanidins reduced the mild hemolytic activity that had been observed for free polyphenols. Consistent with the absence of irritation and hemolysis, the cytotoxicity of the formulations was confirmed by MTT assay

performed on RKO cells of human colorectal carcinoma. The study showed that cell viability was concentration dependent, although after 72 h of incubation even the highest concentrations tested indicated the absence of toxicity [142].

Another treatment for ulcerative colitis was proposed by Wang et al. The authors encapsulated magnolol in core-shell nanoparticles (CS-Zein NPs), consisting of a zein core and a chondroitin sulfate coating, which were in turn embedded in hydrogel microspheres by electrospraying (ES). For comparison, the anionic polysaccharide sodium carboxymethyl cellulose (CUL) was used to replace chondroitin sulfate coating and to prepare untargeted NPs (CUL-Zein NPs). It is known that in ulcerative colitis, inflammation of lesions often occurs in normal colonic epithelial cells and that inflammatory factors are secreted by macrophages [101].

Therefore, normal human colon epithelial cells (NCM 460) and macrophages (Raw 264.7) were selected by the authors to examine cell viability and to determine the concentrations to be tested to assess the anti-inflammatory effect. To determine the anti-inflammatory effects, the two cell lines were stimulated with lipopolysaccharide, and after the incubation period, the amounts of proinflammatory (TNF-α, IL-1β, IL-6) and anti-inflammatory (IL-10) factors in the cell supernatant were determined by ELISA. The results showed that chondroitin sulfate coating enhanced the anti-inflammatory effect. To understand if the superior performance of the coated CS-Zein NPs could be attributed to increased cellular uptake, the fluorescent probe coumarin-6 was encapsulated in the NPs (C6@CS-Zein NPs). Flow cytometry and confocal laser scanning microscopy (CLSM) confirmed the hypothesis that chondroitin sulfate coating enhanced CD44 receptor-mediated endocytosis and consequently the cellular uptake (Figure 17) [143].

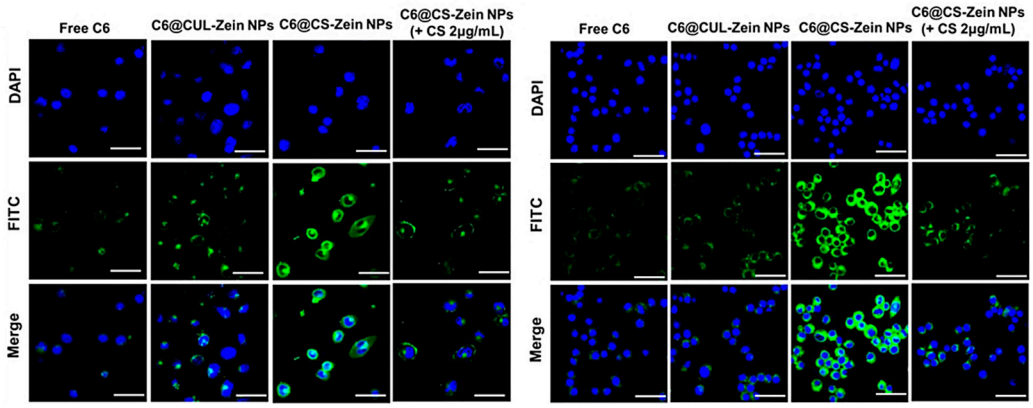

Figure 17. Fluorescence images showing cellular uptake of free C6, C6@CUL-Zein NPs, C6@CS-Zein NPs, and C6@CS-Zein NPs (with 2 μg/mL CS pretreatment) in NCM 460 and raw 264.7 cells for 4 h. Scale bar is 50 μm. Adapted with permission from Ref. [143]. 2021, American Chemical Society.

These two cell lines were also used by Xiao et al. to evaluate the cellular uptake of zein and caseinate NPs loaded with isoliquiritigenin for the treatment of ulcerative colitis. For the in vitro study, NPs were labeled with coumarin-6, and the results of CLSM analysis showed that the encapsulated molecule showed significantly higher cellular uptake compared to the free molecule on both cell lines [144].

Another cell line frequently investigated to assess the absorption of orally administered drugs is the Caco-2 cell line [145].

In a study by Salah et al., Caco-2 cells were stimulated with TNF-α and the anti-inflammatory effects of the formulations were observed following early (stimulus + treatment) and late (stimulus for 24 h followed by treatment) treatments. Although the in vitro permeability study demonstrated effective release of encapsulated curcumin across the epithelial barrier, to obtain more reliable results the authors also investigated absorption on an ex vivo murine colon explant [90].

Inflammation is a process that involves several cell layers and should be considered to improve the predictivity of the results. To accurately simulate the architecture of the human intestinal epithelium, an innovative triple co-culture model was developed that included caco-2 cells, HT29-MTX cells and raji-B cells. The lack of ability to generate mucus is a disadvantage of the caco-2 cell line, so HT29-MTX cells derived from calyciform cells were useful to simulate a more predictable model experimental cell [146].

The Raji B cell line, derived from a human Burkitt's lymphoma, was used to induce differentiation of caco-2 cells into M cells of reduced enzyme activity compared with caco-2 cells in monoculture [147].

This interesting model of in vitro intestinal permeability was employed by Prezotti et al. which prepared mucoadhesive beads of gellan gum for colon-targeted administration of RSV. The permeability results showed that the mucoadhesive carriers significantly reduced the permeability of this compound and prolonged contact with colon cells enhanced its local targeting. Therefore, the triple co-culture model proved to be useful for an accurate reproduction of RSV transport through cell monolayers [148].

Although in vitro models do not consider the cellular homeostasis that governs multiple factors in vivo, they are necessary assays to establish biocompatibility and preliminarily screen the most promising formulations to be tested for in vivo applications.

3.2.2. In Vivo Studies

Once the in vitro tests have been performed and the formulation to be tested in vivo has been selected, the next step is to select the most appropriate animal according to the disease to be studied. Most of the reviewed studies explore the pathogenesis of ulcerative colitis, the modeling of which can be done by the immune method or by chemical stimulation. The latter technique is simple, reproducible and inexpensive and is therefore among the most commonly used methods in research in this field [149].

Mice and rats are the laboratory animals most frequently used to study ulcerative colitis, but differences in gut length have been observed between these two species. Mice have a shorter intestine than rats, plus the latter show a classification more similar to humans. Another advantage of rats is that they are well subject to modeling to recreate disease models, so they are the main experimental animals [150].

Rats with a 2,4,6-trinitrobenzenesulfonic acid (TNBS)-induced colitis model were orally treated with alginate and chitosan nanoparticles loaded with berberine hydrochloride with the aim of evaluating the anti-inflammatory efficacy of the systems. Physiological characteristics of ulcerative colitis such as weight loss, colon weight and length, colon mucosal damage, and spleen index were evaluated. An in vivo study showed that nanosystems in addition to reducing disease activity and colonic mucosal damage are able to improve immunological function [91].

A recently introduced model of ulcerative colitis that is similar to human ulcerative colitis in terms of weight loss, reduced colon length, epithelial ulceration, and inflammatory cell infiltration is that induced by SDS [151].

Mice with this model of ulcerative colitis were used to evaluate the efficacy of binary composite NPs of zein and caseinate loaded with isoliquiritigenin. The fluorescent probe 1,1-dioctadecyl-3,3,3,3-tetramethylindotricarbocyanine iodide (DiR) was encapsulated in the NPs (DiR@NPs) to track colonic biodistribution in vivo. The study suggested that the DiR@NPs were efficiently transported across the intestinal barrier into colonic tissues and that the zein/caseinate shell protected the active molecule, delivering it specifically to the colon inflammatory site (Figure 18).

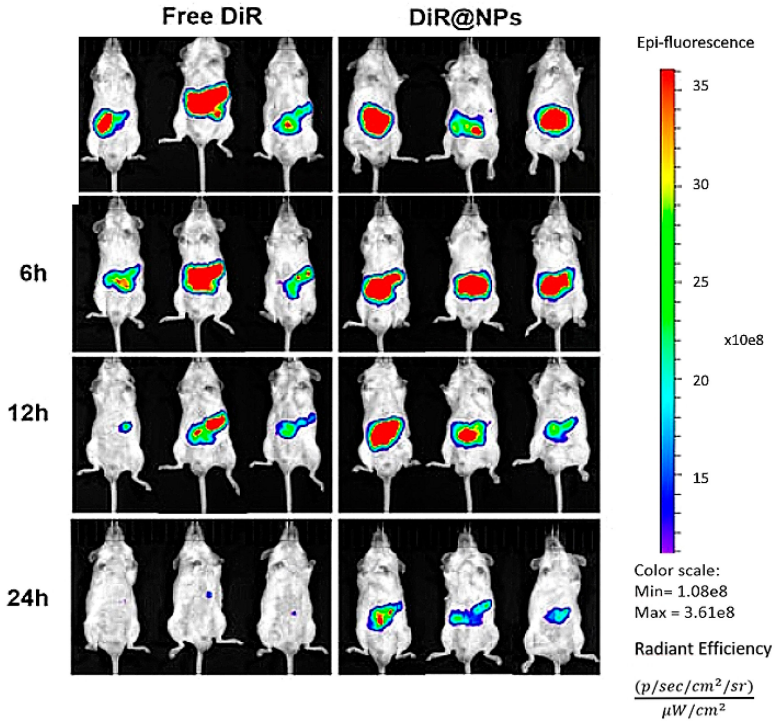

Figure 18. Fluorescence images at different times of mice administered orally with free DiR or DiR@NPs. Adapted with permission from Ref. [144]. 2022, Frontiers Media SA, Lausanne, CH.

Indicators of ulcerative colitis (colonic length, body weight, and DAI scores) were significantly improved following administration of encapsulated isoliquiritigenin. The excellent therapeutic efficacy was further confirmed by the reduction of both pro-inflammatory cytokine levels and neutrophil infiltration in the colonic mucosa, suggesting an advantageous clinical application of these nanosystems in the treatment of ulcerative colitis [144].

The same model of ulcerative colitis was used by Zhang et al. to evaluate the efficacy of a combined formulation for curcumin delivery. This formulation consisted of NPs of zein and hyaluronic acid embedded in hydrogel microparticles prepared from alginate and chitosan. Retention and bioadhesion to colonic tissues were demonstrated by fluorescence imaging after intragastric administration, where the multifunctional platform showed combined advantages over individual systems in delivering curcumin to the colon. Oral administration of the formulation was effective in inhibiting intestinal inflammation (via the TLR4/NF-κB pathway) and consequently alleviating ulcerative colitis symptoms in mice [152].

A mouse model with DDS-induced disease was also employed by Zu et al. to evaluate the efficacy of exosome-like nanotherapeutics produced from tea leaves in delaying the development of IBD and preventing colitis-associated colon cancer. Formulations were produced from small, medium and large tea leaves. Two fluorescent molecules, DiR and 3, 3′-dioctadecylocarboxocyanine perchlorate (DiO), were loaded into the nanomedicines to evaluate biodistribution after oral administration. The results of the study showed that the nanocarriers remained stable in the gastrointestinal tract, and those obtained from large tea leaves showed the best ability to accumulate in inflamed tissues. In addition, the large tea leaf nanotherapeutics were the most effective in mitigating disease symptoms and reducing inflammation and histological lesions in the colon. In mice treated with the large tea leaf nanotherapeutics, the homeostasis of the intestinal microbial population was maintained almost similar to the healthy control group, confirming the retardant effects against IBD. The nanotherapeutics were also found to be effective in inhibiting the development of colon cancer, as they were able to mitigate inflammatory reactions by downregulating the production of proinflammatory cytokines and upregulating IL-10. The proven safety and

efficacy of oral administration make these platforms useful tools for the prevention and treatment of colon diseases [153].

To study diarrhea-predominant irritable bowel syndrome (IBS-D), which is a subtype of IBD, IBS-D model mice induced by chronic restraint stress plus senna alexandrine mill decoction were used. The effects of self-assembled nanoparticles of berberine and baicalin were examined with special focus on the therapeutic influence carried out on the microbiota-gut-brain axis (MGBA) level.

Compared with simple mixing of berberine and baicalin, it was observed that self-assembly of the nanostructures ensured a synergistic effect on IBS-D mice. The nanomedicines improved visceral hypersensitivity, depression, diarrhea and anxious behaviors on IBS-D model mice. In addition, administration by gastric gavage reduced levels of brain-gut peptides (5-hydroxytryptamine, vasoactive intestinal polypeptide, and choline O-acetyltransferase) in colon tissues and serum, confirming the involvement of MGBA in IBS-D. Treatment with NPs reduced the levels of immune inflammation and restored the homeostasis of intestinal flora, which was examined by 16S rRNA gene sequence analysis in microbial samples isolated from the colon. The synergistic effect of nanomedicines involved three different pathways implicated in the onset of IBS-D, providing a potential and efficient platform for therapies of this intestinal disorder [154].

Although in vivo laboratory animal experiments are subject to numerous ethical, regulatory, and economic restrictions, they are necessary tests to demonstrate the impact of a new drug on the whole organism rather than on isolated or co-cultured cells. Global assessment of potential in vivo interactions could improve the predictivity of efficacy and safety of new therapeutic agents while ensuring a realistic estimation of drug candidates to proceed to clinical trials.

4. Conclusions

The use of food-grade polymers in systems for targeted delivery of bioactive substances to the colon is gaining considerable interest in recent years. This approach is particularly useful for improving the bioavailability and efficacy of nutraceuticals, which are known to have beneficial health effects but are often limited by poor absorption and rapid metabolism.

Food polymers, which are nontoxic, biocompatible, and biodegradable, can serve as carriers for bioactive substances and protect them from degradation and premature release in the gastrointestinal tract. This approach may also improve their targeted delivery to the colon, where they can exert their health-promoting effects.

The strategies basing the delivery of drugs in the ileo-colonic region on a single stimulus (i.e., transit time, pH or bacterial enzymes) can be dramatically affected by the large inter- and intra-individual variability that characterize the GIT physiology and, most importantly, its pathological conditions. For this reason, more recently, new formulations which try to subordinate the drug release to two or more physiological stimuli have been proposed [155]. Such a dual or combined (multi-faceted) approach may act sequentially or in parallel. Sequential trigger systems contain for instance two or more layers, each sensitive to different stimuli, e.g., pH and time, that can be activated one after the other and release the entrapped drug along the intestinal tract. Parallel systems instead combine different drug release mechanisms operating simultaneously. One possible advantage is that is one of the mechanisms do not work correctly for a strong physiological variability (e.g., too rapid transit time, abnormal low pH values, or severe disbiosis), the drug release can still be activated by the other mechanism(s).

Multi-stimuli strategies have been mainly applied for the functional coating tablets, pellets and capsules also in colon targeted commercial drugs [156–159]. However, the same principles could be promising also if used for nutraceutical products. Therefore, the expectation from the research in this field is that even new and better-performing associations of food-grade polymers can enter the market, achieving increasingly effective control and efficacy of colon drug delivery.

The technological characterization remains critical in the development of these systems. Morphology, size, surface charge, encapsulation efficiency, and release kinetics are key parameters that can influence their behavior and interaction with biological systems. For example, the size and surface charge of the carrier can affect cellular uptake and adhesion to intestinal epithelium.

The evaluation of stability and biological activity is also of crucial importance in assessing the efficacy and safety of polymer-based carriers and their bioactive cargo. Stability studies can determine the shelf life of the system and its ability to maintain the bioactivity of the loaded substance. Biological activity studies can confirm the therapeutic effects of the delivered bioactive substance and validate the potential of the system in the treatment of gastro-intestinal disorders.

In conclusion, using food-grade polymers to produce new formulations for colon-targeted delivery of bioactive substances is a valid approach to improve the local bioavailability and efficacy of nutraceutical ingredients. Technological characterization and evaluation of stability and biological activity are critical to develop effective and safe products for the treatment of colonic disorders.

Author Contributions: Conceptualization, S.R. and R.P.; writing—original draft preparation, S.R., E.Z., A.R. and R.L.; writing—review and editing, S.R. and R.P.; supervision, R.P. All authors have read and agreed to the published version of the manuscript.

Funding: This research received no external funding.

Institutional Review Board Statement: Not applicable.

Informed Consent Statement: Not applicable.

Conflicts of Interest: The authors declare no conflict of interest.

References

1. Teruel, A.H.; Gonzalez-Alvarez, I.; Bermejo, M.; Merino, V.; Marcos, M.D.; Sancenon, F.; Gonzalez-Alvarez, M.; Martinez-Mañez, R. New Insights of Oral Colonic Drug Delivery Systems for Inflammatory Bowel Disease Therapy. *Int. J. Mol. Sci.* **2020**, *21*, 6502. [CrossRef] [PubMed]
2. Yasmin, F.; Najeeb, H.; Shaikh, S.; Hasanain, M.; Naeem, U.; Moeed, A.; Koritala, T.; Hasan, S.; Surani, S. Novel Drug Delivery Systems for Inflammatory Bowel Disease. *World J. Gastroenterol.* **2022**, *28*, 1922–1933. [CrossRef] [PubMed]
3. Rajpurohit, H.; Sharma, P.; Sharma, S.; Bhandari, A. Polymers for Colon Targeted Drug Delivery. *Indian J. Pharm. Sci.* **2010**, *72*, 689. [CrossRef] [PubMed]
4. Joye, I.J.; Corradini, M.G.; Duizer, L.M.; Bohrer, B.M.; LaPointe, G.; Farber, J.M.; Spagnuolo, P.A.; Rogers, M.A. A Comprehensive Perspective of Food Nanomaterials. *Adv. Food Nutr. Res.* **2019**, *88*, 1–45. [CrossRef]
5. Sarangi, M.K.; Rao, M.E.B.; Parcha, V. Smart Polymers for Colon Targeted Drug Delivery Systems: A Review. *Int. J. Polym. Mater.* **2020**, *70*, 1130–1166. [CrossRef]
6. Arévalo-Pérez, R.; Maderuelo, C.; Lanao, J.M. Recent Advances in Colon Drug Delivery Systems. *J. Control Release* **2020**, *327*, 703–724. [CrossRef]
7. Gazzaniga, A.; Moutaharrik, S.; Filippin, I.; Foppoli, A.; Palugan, L.; Maroni, A.; Cerea, M. Time-Based Formulation Strategies for Colon Drug Delivery. *Pharmaceutics* **2022**, *14*, 2762. [CrossRef]
8. Zhang, L.; McClements, D.J.; Wei, Z.; Wang, G.; Liu, X.; Liu, F. Delivery of Synergistic Polyphenol Combinations Using Biopolymer-Based Systems: Advances in Physicochemical Properties, Stability and Bioavailability. *Crit. Rev. Food Sci. Nutr.* **2020**, *60*, 2083–2097. [CrossRef]
9. Kumar, R.; Islam, T.; Nurunnabi, M. Mucoadhesive Carriers for Oral Drug Delivery. *J. Control. Release* **2022**, *351*, 504–559. [CrossRef]
10. Bakshi, H.A.; Quinn, G.A.; Aljabali, A.A.A.; Hakkim, F.L.; Farzand, R.; Nasef, M.M.; Abuglela, N.; Ansari, P.; Mishra, V.; Serrano-Aroca, Á.; et al. Exploiting the Metabolism of the Gut Microbiome as a Vehicle for Targeted Drug Delivery to the Colon. *Pharmaceuticals* **2021**, *14*, 1211. [CrossRef]
11. Ibrahim, I.M. Advances in Polysaccharide-Based Oral Colon-Targeted Delivery Systems: The Journey So Far and the Road Ahead. *Cureus* **2023**, *15*, e33636. [CrossRef] [PubMed]
12. Balaji, A.B.; Pakalapati, H.; Khalid, M.; Walvekar, R.; Siddiqui, H. Natural and Synthetic Biocompatible and Biodegradable Polymers. In *Biodegradable and Biocompatible Polymer Composites: Processing, Properties and Applications*; Elsevier: Amsterdam, The Netherlands, 2017; Volume 286, pp. 3–32. [CrossRef]

13. Flores-Hernández, C.G.; Cornejo-Villegas, M.d.L.A.; Moreno-Martell, A.; Del Real, A. Del Synthesis of a Biodegradable Polymer of Poly (Sodium Alginate/Ethyl Acrylate). *Polymers* **2021**, *13*, 504. [CrossRef] [PubMed]
14. Paradies, H.H.; Wagner, D.; Fischer, W.R. Multicomponent diffusion of sodium alginate solutions with added salt. II. Charged vs. uncharged system. *Ber. Bunsenges. Phys. Chem.* **1996**, *100*, 1299–1307. [CrossRef]
15. Alirezalu, K.; Yaghoubi, M.; Poorsharif, L.; Aminnia, S.; Kahve, H.I.; Pateiro, M.; Lorenzo, J.M.; Munekata, P.E.S. Antimicrobial Polyamide-Alginate Casing Incorporated with Nisin and ε-Polylysine Nanoparticles Combined with Plant Extract for Inactivation of Selected Bacteria in Nitrite-Free Frankfurter-Type Sausage. *Foods* **2021**, *10*, 1003. [CrossRef]
16. Soares, J.D.P.; Santos, J.E.; Chierice, G.O.; Cavalheiro, E.T.G. Thermal behavior of alginic acid and its sodium salt. *Eclética Química* **2004**, *29*, 57–64. [CrossRef]
17. Mensink, M.A.; Frijlink, H.W.; Van Der Voort Maarschalk, K.; Hinrichs, W.L.J. Inulin, a Flexible Oligosaccharide I: Review of Its Physicochemical Characteristics. *Carbohydr. Polym.* **2015**, *130*, 405–419. [CrossRef]
18. Cao, T.L.; Yang, S.Y.; Song, K. Bin Development of Burdock Root Inulin/Chitosan Blend Films Containing Oregano and Thyme Essential Oils. *Int. J. Mol. Sci.* **2018**, *19*, 131. [CrossRef]
19. de Gennaro, S.; Birch, G.G.; Parke, S.A.; Stancher, B. Studies on the physicochemical properties of inulin and inulin oligomers. *Food Chem.* **2000**, *68*, 179–183. [CrossRef]
20. Leyva-Porras, C.; Saavedra–Leos, M.Z.; López-Pablos, A.L.; Soto-Guerrero, J.J.; Toxqui-Terán, A.; Fozado-Quiroz, R.E. Chemical, Thermal and Physical Characterization of Inulin for Its Technological Application Based on the Degree of Polymerization. *J. Food Process. Eng.* **2017**, *40*, e12333. [CrossRef]
21. El-Kholy, W.M.; Aamer, R.A.; Ali, A.N.A. Utilization of Inulin Extracted from Chicory (*Cichorium Intybus* L.) Roots to Improve the Properties of Low-Fat Synbiotic Yoghurt. *Ann. Agric. Sci.* **2020**, *65*, 59–67. [CrossRef]
22. Miranda, S.P.; Garnica, O.; Lara-Sagahon, V.; Cárdenas, G. Water Vapor Permeability and Mechanical Properties of Chitosan Composite Films. *J. Chil. Chem. Soc.* **2004**, *49*, 173–178. [CrossRef]
23. Szymańska, E.; Winnicka, K. Stability of Chitosan-A Challenge for Pharmaceutical and Biomedical Applications. *Mar. Drugs* **2015**, *13*, 1819–1846. [CrossRef] [PubMed]
24. Wang, S.T.; Tsai, C.C.; Shih, M.C.; Tsai, M.L. Flavor-Related Applications of Chitin and Chitosan in Foods: Effect of Structure and Properties on the Efficacy. In *Advances in Polymer Science*; Springer Science and Business Media Deutschland GmbH: Berlin, Germany, 2021; Volume 287, pp. 169–202. [CrossRef]
25. Georgieva, V.; Zvezdova, D.; Vlaev, L. Non-isothermal kinetics of thermal degradation of chitosan. *Chem. Cent. J.* **2012**, *6*, 1–10. [CrossRef] [PubMed]
26. Diaz, J.V.; Anthon, G.E.; Barrett, D.M. Nonenzymatic Degradation of Citrus Pectin and Pectate during Prolonged Heating: Effects of PH, Temperature, and Degree of Methyl Esterification. *J. Agric. Food Chem.* **2007**, *55*, 5131–5136. [CrossRef] [PubMed]
27. Basu, S.; Shivhare, U.S.; Muley, S. Moisture Adsorption Isotherms and Glass Transition Temperature of Pectin. *J. Food Sci. Technol.* **2013**, *50*, 585–589. [CrossRef] [PubMed]
28. Saikia, M.; Badwaik, L.S. Characterization and Antimicrobial Property of Casein, Gelatin and Pectin Based Active Composite Films. *J. Packag. Technol. Res.* **2018**, *2*, 233–242. [CrossRef]
29. Nesic, A.; Meseldzija, S.; Cabrera-Barjas, G.; Onjia, A. Novel Biocomposite Films Based on High Methoxyl Pectin Reinforced with Zeolite Y for Food Packaging Applications. *Foods* **2022**, *11*, 360. [CrossRef]
30. Chen, Y.; Ye, R.; Liu, J. Effects of Different Concentrations of Ethanol and Isopropanol on Physicochemical Properties of Zein-Based Films. *Ind. Crops Prod.* **2014**, *53*, 140–147. [CrossRef]
31. Pérez-Guzmán, C.J.; Castro-Muñoz, R. A Review of Zein as a Potential Biopolymer for Tissue Engineering and Nanotechnological Applications. *Processes* **2020**, *8*, 1376. [CrossRef]
32. Zhang, L.; Liu, Z.; Sun, Y.; Wang, X.; Li, L. Effect of α-Tocopherol Antioxidant on Rheological and Physicochemical Properties of Chitosan/Zein Edible Films. *LWT* **2020**, *118*, 108799. [CrossRef]
33. Rezaei, A.; Tavanai, H.; Nasirpour, A. Fabrication of Electrospun Almond Gum/PVA Nanofibers as a Thermostable Delivery System for Vanillin. *Int. J. Biol. Macromol.* **2016**, *91*, 536–543. [CrossRef] [PubMed]
34. Tahsiri, Z.; Mirzaei, H.; Hosseini, S.M.H.; Khalesi, M. Gum Arabic Improves the Mechanical Properties of Wild Almond Protein Film. *Carbohydr. Polym.* **2019**, *222*, 114994. [CrossRef]
35. Farooq, U.; Sharma, K.; Malviya, R. Extraction and Characterization of Almond (Prunus Sulcis) Gum as Pharmaceutical Excipient. *J. Agric. Environ. Sci.* **2014**, *14*, 269–274. [CrossRef]
36. Seck, M.; Diallo, A.K.; Erouel, M.; Saadi, M.; Tiss, B.; Wederni, M.A.; Tall, A.; Babacar Ly, E.H.; Kobor, D.; Bouguila, N.; et al. Dielectric Investigation and Material Properties of Almond Gum Thin Films Deposited by Spray Pyrolysis. *Mater. Chem. Phys.* **2021**, *272*, 124917. [CrossRef]
37. Bouaziz, F.; Helbert, C.B.; Ben Romdhane, M.; Koubaa, M.; Bhiri, F.; Kallel, F.; Chaari, F.; Driss, D.; Buon, L.; Chaabouni, S.E. Structural Data and Biological Properties of Almond Gum Oligosaccharide: Application to Beef Meat Preservation. *Int. J. Biol. Macromol.* **2014**, *72*, 472–479. [CrossRef] [PubMed]
38. Alvarado-González, J.S.; Chanona-Pérez, J.J.; Welti-Chanes, J.S.; Calderón-Domínguez, G.; Arzate-Vázquez, I.; Pacheco-Alcalá, S.U.; Garibay-Febles, V.; Gutiérrez-López, G.F. Optical, microstructural, functional and nanomechanical properties of Aloe vera gel/gellan gum edible films. *Rev. Mex. Ing. Química* **2012**, *11*, 193–210.

39. Omoto, T.; Uno, Y.; Asai, I. The latest technologies for the application of gellan gum. In *Physical Chemistry and Industrial Application of Gellan Gum*; Springer: Berlin/Heidelberg, Germany, 1999; Volume 114, pp. 123–126. [CrossRef]
40. EUDRAGUARD®Portfolio of Supplement Coatings. Available online: https://healthcare.evonik.com/en/nutrition/supplement-coatings/eudraguard-portfolio (accessed on 8 March 2023).
41. Curcio, C.; Greco, A.S.; Rizzo, S.; Saitta, L.; Musumeci, T.; Ruozi, B.; Pignatello, R. Development, Optimization and Characterization of Eudraguard®-Based Microparticles for Colon Delivery. *Pharmaceuticals* **2020**, *13*, 131. [CrossRef] [PubMed]
42. Weinberger, H.; Gardner, W.H. Chemical composition of shellac. *Ind. Eng. Chem.* **1938**, *30*, 454–458. [CrossRef]
43. Sameni, J.; Krigstin, S.; Sain, M. Solubility of lignin and acetylated lignin in organic solvents. *BioResources* **2017**, *12*, 1548–1565. [CrossRef]
44. Guggenberger, M.; Sumerskii, I.; Rosenau, T.; Böhmdorfer, S.; Potthast, A. The Return of the Smell: The Instability of Lignin's Odor. *ACS Sustain. Chem. Eng.* **2023**, *11*, 689–695. [CrossRef]
45. Dhamecha, D.; Movsas, R.; Sano, U.; Menon, J.U. Applications of Alginate Microspheres in Therapeutics Delivery and Cell Culture: Past, Present and Future. *Int. J. Pharm.* **2019**, *569*, 118627. [CrossRef] [PubMed]
46. Yu, L.; Sun, Q.; Hui, Y.; Seth, A.; Petrovsky, N.; Zhao, C.X. Microfluidic Formation of Core-Shell Alginate Microparticles for Protein Encapsulation and Controlled Release. *J. Colloid Interface Sci.* **2019**, *539*, 497–503. [CrossRef] [PubMed]
47. Sinha, V.R.; Singla, A.K.; Wadhawan, S.; Kaushik, R.; Kumria, R.; Bansal, K.; Dhawan, S. Chitosan Microspheres as a Potential Carrier for Drugs. *Int. J. Pharm.* **2004**, *274*, 1–33. [CrossRef] [PubMed]
48. El Kadib, A. Green and Functional Aerogels by Macromolecular and Textural Engineering of Chitosan Microspheres. *Chem. Rec.* **2020**, *20*, 753–772. [CrossRef]
49. Jafernik, K.; Ładniak, A.; Blicharska, E.; Czarnek, K.; Ekiert, H.; Wiącek, A.E.; Szopa, A. Chitosan-Based Nanoparticles as Effective Drug Delivery Systems-A Review. *Molecules* **2023**, *28*, 1963. [CrossRef]
50. Tie, S.; Su, W.; Zhang, X.; Chen, Y.; Zhao, X.; Tan, M. PH-Responsive Core-Shell Microparticles Prepared by a Microfluidic Chip for the Encapsulation and Controlled Release of Procyanidins. *J. Agric. Food Chem.* **2021**, *69*, 1466–1477. [CrossRef] [PubMed]
51. Paliwal, R.; Palakurthi, S. Zein in Controlled Drug Delivery and Tissue Engineering. *J. Control. Release* **2014**, *189*, 108–122. [CrossRef]
52. Hu, Q.; Bae, M.; Fleming, E.; Lee, J.Y.; Luo, Y. Biocompatible Polymeric Nanoparticles with Exceptional Gastrointestinal Stability as Oral Delivery Vehicles for Lipophilic Bioactives. *Food Hydrocoll.* **2019**, *89*, 386–395. [CrossRef]
53. Wei, Y.; Guo, A.; Liu, Z.; Mao, L.; Yuan, F.; Gao, Y.; Mackie, A. Structural Design of Zein-Cellulose Nanocrystals Core–Shell Microparticles for Delivery of Curcumin. *Food Chem.* **2021**, *357*, 129849. [CrossRef]
54. Kedir, W.M.; Deresa, E.M.; Diriba, T.F. Pharmaceutical and Drug Delivery Applications of Pectin and Its Modified Nanocomposites. *Heliyon* **2022**, *8*, e10654. [CrossRef]
55. Mohnen, D. Pectin Structure and Biosynthesis. *Curr. Opin. Plant Biol.* **2008**, *11*, 266–277. [CrossRef] [PubMed]
56. Khotimchenko, M. Pectin Polymers for Colon-Targeted Antitumor Drug Delivery. *Int. J. Biol. Macromol.* **2020**, *158*, 1110–1124. [CrossRef] [PubMed]
57. Lee, T.; Chang, Y.H. Structural, Physicochemical, and In-Vitro Release Properties of Hydrogel Beads Produced by Oligochitosan and de-Esterified Pectin from Yuzu (Citrus Junos) Peel as a Quercetin Delivery System for Colon Target. *Food Hydrocoll.* **2020**, *108*, 106086. [CrossRef]
58. Giri, S.; Dutta, P.; Giri, T.K. Inulin-Based Carriers for Colon Drug Targeting. *J. Drug Deliv. Sci. Technol.* **2021**, *64*, 102595. [CrossRef]
59. Wang, D.; Sun, F.; Lu, C.; Chen, P.; Wang, Z.; Qiu, Y.; Mu, H.; Miao, Z.; Duan, J. Inulin Based Glutathione-Responsive Delivery System for Colon Cancer Treatment. *Int. J. Biol. Macromol.* **2018**, *111*, 1264–1272. [CrossRef] [PubMed]
60. Yuan, Y.; He, N.; Dong, L.; Guo, Q.; Zhang, X.; Li, B.; Li, L. Multiscale Shellac-Based Delivery Systems: From Macro: From Nanoscale. *ACS Nano* **2021**, *15*, 18794–18821. [CrossRef] [PubMed]
61. Yuan, Y.; Li, H.; Zhu, J.; Liu, C.; Sun, X.; Wang, D.; Xu, Y. Fabrication and Characterization of Zein Nanoparticles by Dextran Sulfate Coating as Vehicles for Delivery of Curcumin. *Int. J. Biol. Macromol.* **2020**, *151*, 1074–1083. [CrossRef]
62. Wang, X.; Yu, D.G.; Li, X.Y.; Bligh, S.W.A.; Williams, G.R. Electrospun Medicated Shellac Nanofibers for Colon-Targeted Drug Delivery. *Int. J. Pharm.* **2015**, *490*, 384–390. [CrossRef]
63. Lauro, M.R.; Picerno, P.; Franceschelli, S.; Pecoraro, M.; Aquino, R.P.; Pignatello, R. Eudraguard® Natural and Protect: New "Food Grade" Matrices for the Delivery of an Extract from Sorbus Domestica L. Leaves Active on the α-Glucosidase Enzyme. *Pharmaceutics* **2023**, *15*, 295. [CrossRef]
64. EUDRAGIT®Functional Polymers for Oral Solid Dosage Forms. Available online: https://healthcare.evonik.com/en/drugdelivery/oral-drug-delivery/oral-excipients/eudragit-portfolio (accessed on 8 March 2023).
65. Curcio, C.; Bonaccorso, A.; Musumeci, T.; Pignatello, R. Oral Controlled Delivery of Natural Compounds Using Food-Grade Polymer Microparticles. *Curr. Nutraceuticals* **2020**, *2*, 145–153. [CrossRef]
66. Yus, C.; Gracia, R.; Larrea, A.; Andreu, V.; Irusta, S.; Sebastian, V.; Mendoza, G.; Arruebo, M. Targeted Release of Probiotics from Enteric Microparticulated Formulations. *Polymers* **2019**, *11*, 1668. [CrossRef] [PubMed]
67. Verma, D.; Sharma, S.K. Recent Advances in Guar Gum Based Drug Delivery Systems and Their Administrative Routes. *Int. J. Biol. Macromol.* **2021**, *181*, 653–671. [CrossRef] [PubMed]
68. Soleimani, K.; Derakhshankhah, H.; Jaymand, M.; Samadian, H. Stimuli-Responsive Natural Gums-Based Drug Delivery Systems for Cancer Treatment. *Carbohydr. Polym.* **2021**, *254*, 117422. [CrossRef] [PubMed]

69. Sagbas, S.; Sahiner, N. Modifiable Natural Gum Based Microgel Capsules as Sustainable Drug Delivery Systems. *Carbohydr. Polym.* **2018**, *200*, 128–136. [CrossRef]
70. Palumbo, F.S.; Federico, S.; Pitarresi, G.; Fiorica, C.; Giammona, G. Gellan Gum-Based Delivery Systems of Therapeutic Agents and Cells. *Carbohydr. Polym.* **2020**, *229*, 115430. [CrossRef] [PubMed]
71. Jadav, M.; Pooja, D.; Adams, D.J.; Kulhari, H. Advances in Xanthan Gum-Based Systems for the Delivery of Therapeutic Agents. *Pharmaceutics* **2023**, *15*, 402. [CrossRef] [PubMed]
72. Bhosale, R.R.; Gangadharappa, H.V.; Osmani, R.A.M.; Gowda, D.V. Design and Development of Polymethylmethacrylate-Grafted Gellan Gum (PMMA-g-GG)-Based PH-Sensitive Novel Drug Delivery System for Antidiabetic Therapy. *Drug Deliv. Transl. Res.* **2020**, *10*, 1002–1018. [CrossRef]
73. Hashemi, K.; Hosseini, E. The Stabilizing and Prebiotic Potential of Water-Soluble Phase of Bitter Almond Gum Exudate in Probiotic Yogurt Drink. *Carbohydr. Polym.* **2021**, *255*, 117395. [CrossRef]
74. Venkatesan, R.; Sekar, S.; Raorane, C.J.; Raj, V.; Kim, S.C. Hydrophilic Composites of Chitosan with Almond Gum: Characterization and Mechanical, and Antimicrobial Activity for Compostable Food Packaging. *Antibiotics* **2022**, *11*, 1502. [CrossRef]
75. Amani, F.; Rezaei, A.; Damavandi, M.S.; Doost, A.S.; Jafari, S.M. Colloidal Carriers of Almond Gum/Gelatin Coacervates for Rosemary Essential Oil: Characterization and in-Vitro Cytotoxicity. *Food Chem.* **2022**, *377*, 131998. [CrossRef]
76. Kanteti, R.V.; Sarheed, O.; Yadav, H.; Islam, Q.; Boateng, J. Studies on Almond Gum and Gelucire-Based Pellets Prepared by Extrusion and Spheronization for Sustained Release. *Turk. J. Pharm. Sci.* **2022**, *19*, 521–529. [CrossRef] [PubMed]
77. Salehi, A.; Rezaei, A.; Damavandi, M.S.; Kharazmi, M.S.; Jafari, S.M. Almond Gum-Sodium Caseinate Complexes for Loading Propolis Extract: Characterization, Antibacterial Activity, Release, and In-Vitro Cytotoxicity. *Food Chem.* **2023**, *405*, 134801. [CrossRef] [PubMed]
78. Oliveira, A.L.C.d.S.L.; Schomann, T.; de Geus-Oei, L.-F.; Kapiteijn, E.; Cruz, L.J.; Junior, R.F.d.A. Nanocarriers as a Tool for the Treatment of Colorectal Cancer. *Pharmaceutics* **2021**, *13*, 1321. [CrossRef] [PubMed]
79. Liu, S.; Fang, Z.; Ng, K. Incorporating Inulin and Chitosan in Alginate-Based Microspheres for Targeted Delivery and Release of Quercetin to Colon. *Food Res. Int.* **2022**, *160*, 111749. [CrossRef]
80. Rizzo, S.; Cosentino, G.; Zingale, E.; Bonaccorso, A.; Petralia, S.; Monforte, F.; Condorelli, G.G.; Carbone, C.; Pignatello, R. Microscopic Evidence of the Behavior of PH-Sensitive Food-Grade Polymeric Delivery Systems. *Curr. Nutraceuticals* **2023**, *4*. pressview.
81. Sarma, S.; Agarwal, S.; Bhuyan, P.; Hazarika, J.; Ganguly, M. Resveratrol-Loaded Chitosan-Pectin Core-Shell Nanoparticles as Novel Drug Delivery Vehicle for Sustained Release and Improved Antioxidant Activities. *R. Soc. Open Sci.* **2022**, *9*, 210784. [CrossRef]
82. Tizro, P.; Choi, C.; Khanlou, N. Sample Preparation for Transmission Electron Microscopy. In *Methods in Molecular Biology*; Humana Press Inc.: Totowa, NJ, USA, 2019; Volume 1897, pp. 417–424. [CrossRef]
83. Kulbacka, J.; Wilk, K.A.; Bazylińska, U.; Dubińska-Magiera, M.; Potoczek, S.; Saczko, J. Curcumin Loaded Nanocarriers with Varying Charges Augmented with Electroporation Designed for Colon Cancer Therapy. *Int. J. Mol. Sci.* **2022**, *23*, 1377. [CrossRef]
84. Wang, D.; Sha, L.; Xu, C.; Huang, Y.; Tang, C.; Xu, T.; Li, X.; Di, D.; Liu, J.; Yang, L. Natural Saponin and Cholesterol Assembled Nanostructures as the Promising Delivery Method for Saponin. *Colloids Surf. B Biointerfaces* **2022**, *214*, 112448. [CrossRef]
85. Bootz, A.; Vogel, V.; Schubert, D.; Kreuter, J. Comparison of Scanning Electron Microscopy, Dynamic Light Scattering and Analytical Ultracentrifugation for the Sizing of Poly(Butyl Cyanoacrylate) Nanoparticles. *Eur. J. Pharm. Biopharm.* **2004**, *57*, 369–375. [CrossRef]
86. Doost, S.A.; Kassozi, V.; Grootaert, C.; Claeys, M.; Dewettinck, K.; van Camp, J.; van der Meeren, P. Self-Assembly, Functionality, and in-Vitro Properties of Quercetin Loaded Nanoparticles Based on Shellac-Almond Gum Biological Macromolecules. *Int. J. Biol. Macromol.* **2019**, *129*, 1024–1033. [CrossRef]
87. Lu, L.; Chen, G.; Qiu, Y.; Li, M.; Liu, D.; Hu, D.; Gu, X.; Xiao, Z. Nanoparticle-Based Oral Delivery Systems for Colon Targeting: Principles and Design Strategies. *Sci. Bull.* **2016**, *61*, 670–681. [CrossRef]
88. Kumar, S.C.; Thangam, R.; Mary, S.A.; Kannan, P.R.; Arun, G.; Madhan, B. Targeted Delivery and Apoptosis Induction of Trans-Resveratrol-Ferulic Acid Loaded Chitosan Coated Folic Acid Conjugate Solid Lipid Nanoparticles in Colon Cancer Cells. *Carbohydr. Polym.* **2020**, *231*, 115682. [CrossRef] [PubMed]
89. Maisel, K.; Ensign, L.; Reddy, M.; Cone, R.; Hanes, J. Effect of Surface Chemistry on Nanoparticle Interaction with Gastrointestinal Mucus and Distribution in the Gastrointestinal Tract Following Oral and Rectal Administration in the Mouse. *J. Control Release* **2015**, *197*, 48–57. [CrossRef] [PubMed]
90. Salah, N.; Dubuquoy, L.; Carpentier, R.; Betbeder, D. Starch Nanoparticles Improve Curcumin-Induced Production of Anti-Inflammatory Cytokines in Intestinal Epithelial Cells. *Int. J. Pharm. X* **2022**, *4*, 100114. [CrossRef]
91. Mohanbhai, S.J.; Sardoiwala, M.N.; Gupta, S.; Shrimali, N.; Choudhury, S.R.; Sharma, S.S.; Guchhait, P.; Karmakar, S. Colon Targeted Chitosan-Melatonin Nanotherapy for Preclinical Inflammatory Bowel Disease. *Biomater. Adv.* **2022**, *136*, 212796. [CrossRef] [PubMed]
92. Sun, L.; Nie, X.; Lu, W.; Zhang, Q.; Fang, W.; Gao, S.; Chen, S.; Hu, R. Mucus-Penetrating Alginate-Chitosan Nanoparticles Loaded with Berberine Hydrochloride for Oral Delivery to the Inflammation Site of Ulcerative Colitis. *AAPS PharmSciTech* **2022**, *23*, 179. [CrossRef] [PubMed]
93. Alkhader, E.; Billa, N.; Roberts, C.J. Mucoadhesive Chitosan-Pectinate Nanoparticles for the Delivery of Curcumin to the Colon. *AAPS PharmSciTech* **2017**, *18*, 1009–1018. [CrossRef] [PubMed]

94. Wang, W.; Yan, X.; Li, Q.; Chen, Z.; Wang, Z.; Hu, H. Adapted nano-carriers for gastrointestinal defense components: Surface strategies and challenges. *Nanomed. Nanotechnol. Biol. Med.* **2020**, *29*, 102277. [CrossRef] [PubMed]
95. Abbas, Q.; Yousaf, B.; Amina; Ali, M.U.; Munir, M.A.M.; El-Naggar, A.; Rinklebe, J.; Naushad, M. Transformation Pathways and Fate of Engineered Nanoparticles (ENPs) in Distinct Interactive Environmental Compartments: A Review. *Environ. Int.* **2020**, *138*, 105646. [CrossRef] [PubMed]
96. Wang, T.X.; Li, X.X.; Chen, L.; Li, L.; Janaswamy, S. Carriers Based on Zein-Dextran Sulfate Sodium Binary Complex for the Sustained Delivery of Quercetin. *Front. Chem.* **2020**, *8*, 662. [CrossRef]
97. Wang, X.; Peng, F.; Liu, F.; Xiao, Y.; Li, F.; Lei, H.; Wang, J.; Li, M.; Xu, H. Zein-Pectin Composite Nanoparticles as an Efficient Hyperoside Delivery System: Fabrication, Characterization, and in Vitro Release Property. *LWT* **2020**, *133*, 109869. [CrossRef]
98. Yun, P.; Devahastin, S.; Chiewchan, N. Microstructures of Encapsulates and Their Relations with Encapsulation Efficiency and Controlled Release of Bioactive Constituents: A Review. *Compr. Rev. Food Sci. Food Saf.* **2021**, *20*, 1768–1799. [CrossRef] [PubMed]
99. Sorasitthiyanukarn, F.N.; Ratnatilaka Na Bhuket, P.; Muangnoi, C.; Rojsitthisak, P.; Rojsitthisak, P. Chitosan/Alginate Nanoparticles as a Promising Carrier of Novel Curcumin Diethyl Diglutarate. *Int. J. Biol. Macromol.* **2019**, *131*, 1125–1136. [CrossRef] [PubMed]
100. Kurra, P.; Narra, K.; Puttugunta, S.B.; Kilaru, N.B.; Mandava, B.R. Development and Optimization of Sustained Release Mucoadhesive Composite Beads for Colon Targeting. *Int. J. Biol. Macromol.* **2019**, *139*, 320–331. [CrossRef]
101. Zhang, S.; Kang, L.; Hu, S.; Hu, J.; Fu, Y.; Hu, Y.; Yang, X. Carboxymethyl Chitosan Microspheres Loaded Hyaluronic Acid/Gelatin Hydrogels for Controlled Drug Delivery and the Treatment of Inflammatory Bowel Disease. *Int. J. Biol. Macromol.* **2021**, *167*, 1598–1612. [CrossRef]
102. Karakas, C.Y.; Ordu, H.R.; Bozkurt, F.; Karadag, A. Electrosprayed Chitosan-Coated Alginate–Pectin Beads as Potential System for Colon-Targeted Delivery of Ellagic Acid. *J. Sci. Food Agric.* **2022**, *102*, 965–975. [CrossRef]
103. Agarwal, T.; Narayana, S.G.H.; Pal, K.; Pramanik, K.; Giri, S.; Banerjee, I. Calcium alginate-carboxymethyl cellulose beads for colon-targeted drug delivery. *Int. J. Biol. Macromol.* **2015**, *75*, 409–417. [CrossRef]
104. Kulsoom, R.; Sarfraz, M.; Afzal, A.; Farooq, M.; Adnan, S.; Ashraf, M.U.; Khan, S.A. Synthesis of Calcium Carbonate-Quince Bio-Composite for Programmed and on-Demand Drug Release of Paracetamol at Target Site: A Green Chemistry Approach. *Polym. Bull.* **2022**, *30*, 1–24. [CrossRef]
105. Ullah, K.; Khan, S.A.; Murtaza, G.; Sohail, M.; Manan, A.; Afzal, A. Gelatin-based hydrogels as potential biomaterials for colonic delivery of oxaliplatin. *Int. J. Pharm.* **2019**, *556*, 236–245. [CrossRef]
106. Natrajan, D.; Srinivasan, S.; Sundar, K.; Ravindran, A. Formulation of Essential Oil-Loaded Chitosan-Alginate Nanocapsules. *J. Food Drug Anal.* **2015**, *23*, 560–568. [CrossRef]
107. Jangid, A.K.; Solanki, R.; Patel, S.; Pooja, D.; Kulhari, H. Genistein Encapsulated Inulin-Stearic Acid Bioconjugate Nanoparticles: Formulation Development, Characterization and Anticancer Activity. *Int. J. Biol. Macromol.* **2022**, *206*, 213–221. [CrossRef]
108. Ali, H.E.; Radwan, R.R. Synthesis, Characterization and Evaluation of Resveratrol-Loaded Functionalized Carbon Nanotubes as a Novel Delivery System in Radiation Enteropathy. *Eur. J. Pharm. Sci.* **2021**, *167*, 106002. [CrossRef]
109. Yingying, M.; Xiu-Xia, L.; Luyun, C.; Jianrong, L. PH-Sensitive ϵ-Polylysine/Polyaspartic Acid/Zein Nanofiber Membranes for the Targeted Release of Polyphenols. *Food Funct.* **2022**, *13*, 6792–6801. [CrossRef] [PubMed]
110. Wasay, S.A.; Jan, S.U.; Akhtar, M.; Noreen, S.; Gul, R. Developed Meloxicam Loaded Microparticles for Colon Targeted Delivery: Statistical Optimization, Physicochemical Characterization, and in-Vivo Toxicity Study. *PLoS ONE* **2022**, *17*, e0267306. [CrossRef] [PubMed]
111. Doost, S.A.; Muhammad, D.R.A.; Stevens, C.V.; Dewettinck, K.; van der Meeren, P. Fabrication and Characterization of Quercetin Loaded Almond Gum-Shellac Nanoparticles Prepared by Antisolvent Precipitation. *Food Hydrocoll.* **2018**, *83*, 190–201. [CrossRef]
112. Shirmohammadli, F.; Nikzad, M.; Ghoreyshi, A.A.; Mohammadi, M.; Poureini, F. Preparation and Characterization of Zein/Sodium Caseinate/Xanthan Gum Complex for Encapsulation of Piperine and Its In Vitro Release Study. *Food Biophys.* **2021**, *16*, 254–269. [CrossRef]
113. Jain, A.K.; Thareja, S. In Vitro and in Vivo Characterization of Pharmaceutical Nanocarriers Used for Drug Delivery. *Artif. Cells Nanomed. Biotechnol.* **2019**, *47*, 524–539. [CrossRef] [PubMed]
114. Lima, L.C.B.; Coelho, C.C.; Silva, F.C.; Meneguin, A.B.; Barud, H.S.; Bezerra, R.D.S.; Viseras, C.; Osajima, J.A.; Silva-Filho, E.C. Hybrid Systems Based on Talc and Chitosan for Controlled Drug Release. *Materials* **2019**, *12*, 3634. [CrossRef]
115. Zhang, X.; Han, Y.; Huang, W.; Jin, M.; Gao, Z. The Influence of the Gut Microbiota on the Bioavailability of Oral Drugs. *Acta Pharm. Sin. B* **2021**, *11*, 1789–1812. [CrossRef]
116. Hanmantrao, M.; Chaterjee, S.; Kumar, R.; Vishwas, S.; Harish, V.; Porwal, O.; Alrouji, M.; Alomeir, O.; Alhajlah, S.; Gulati, M.; et al. Development of Guar Gum-Pectin-Based Colon Targeted Solid Self-Nanoemulsifying Drug Delivery System of Xanthohumol. *Pharmaceutics* **2022**, *14*, 2384. [CrossRef]
117. Bermejo, M.; Sanchez-Dengra, B.; Gonzalez-Alvarez, M.; Gonzalez-Alvarez, I. Oral Controlled Release Dosage Forms: Dissolution versus Diffusion. *Expert Opin. Drug Deliv.* **2020**, *17*, 791–803. [CrossRef] [PubMed]
118. Wang, S.; Liu, R.; Fu, Y.; Kao, W.J. Release Mechanisms and Applications of Drug Delivery Systems for Extended-Release. *Expert Opin. Drug Deliv.* **2020**, *17*, 1289–1304. [CrossRef]

119. Tang, X.F.; Zhang, X.Y.; Zhao, Q.Q. A PH/Time/Pectinase-Dependent Oral Colon-Targeted System Containing Isoliquiritigenin: Pharmacokinetics and Colon Targeting Evaluation in Mice. *Eur. J. Drug Metab. Pharmacokinet.* **2022**, *47*, 677–686. [CrossRef] [PubMed]
120. Hens, B.; Sinko, P.; Job, N.; Dean, M.; Al-Gousous, J.; Salehi, N.; Ziff, R.M.; Tsume, Y.; Bermejo, M.; Paixão, P.; et al. Formulation Predictive Dissolution (FPD) Testing to Advance Oral Drug Product Development: An Introduction to the US FDA Funded '21st Century BA/BE' Project. *Int. J. Pharm.* **2018**, *548*, 120–127. [CrossRef] [PubMed]
121. Ruiz-Picazo, A.; Lozoya-Agullo, I.; González-Álvarez, I.; Bermejo, M.; González-Álvarez, M. Effect of Excipients on Oral Absorption Process According to the Different Gastrointestinal Segments. *Expert Opin. Drug Deliv.* **2021**, *18*, 1005–1024. [CrossRef]
122. Silchenko, S.; Nessah, N.; Li, J.; Li, L.-B.; Huang, Y.; Owen, A.J.; Hidalgo, I.J. In Vitro Dissolution Absorption System (IDAS2): Use for the Prediction of Food Viscosity Effects on Drug Dissolution and Absorption from Oral Solid Dosage Forms. *Eur. J. Pharm. Sci.* **2020**, *143*, 105164. [CrossRef]
123. Andishmand, H.; Tabibiazar, M.; Mohammadifar, M.A.; Hamishehkar, H. Pectin-Zinc-Chitosan-Polyethylene Glycol Colloidal Nano-Suspension as a Food Grade Carrier for Colon Targeted Delivery of Resveratrol. *Int. J. Biol. Macromol.* **2017**, *97*, 16–22. [CrossRef]
124. Zhang, C.; Chen, Z.; He, Y.; Xian, J.; Luo, R.; Zheng, C.; Zhang, J. Oral Colon-Targeting Core–Shell Microparticles Loading Curcumin for Enhanced Ulcerative Colitis Alleviating Efficacy. *Chin. Med.* **2021**, *16*, 92. [CrossRef]
125. Wang, X.; Xie, H.; Shi, C.; Dziugan, P.; Zhao, H.; Zhang, B. Fabrication and Characterization of Gel Beads of Whey Isolate Protein–Pectin Complex for Loading Quercetin and Their Digestion Release. *Gels* **2022**, *8*, 18. [CrossRef]
126. Feng, X.; Xie, Q.; Xu, H.; Zhang, T.; Li, X.; Tian, Y.; Lan, H.; Kong, L.; Zhang, Z. Yeast Microcapsule Mediated Natural Products Delivery for Treating Ulcerative Colitis through Anti-Inflammatory and Regulation of Macrophage Polarization. *ACS Appl. Mater. Interfaces* **2022**, *14*, 31085–31098. [CrossRef]
127. Boukoufi, C.; Boudier, A.; Maincent, P.; Vigneron, J.; Clarot, I. Food-Inspired Innovations to Improve the Stability of Active Pharmaceutical Ingredients. *Int. J. Pharm.* **2022**, *623*, 121881. [CrossRef] [PubMed]
128. Pramar, Y.V.; Mandal, T.K.; Bostanian, L.A.; Le, G.; Morris, T.C.; Graves, R.A. Physicochemical and Microbiological Stability of Compounded Metronidazole Suspensions in PCCA SuspendIt. *Int. J. Pharm. Compd.* **2021**, *25*, 169. [PubMed]
129. González-González, O.; Ramirez, I.O.; Ramirez, B.I.; O'Connell, P.; Ballesteros, M.P.; Torrado, J.J.; Serrano, D.R. Drug Stability: ICH versus Accelerated Predictive Stability Studies. *Pharmaceutics* **2022**, *14*, 2324. [CrossRef] [PubMed]
130. Shao, P.; Feng, J.; Sun, P.; Xiang, N.; Lu, B.; Qiu, D. Recent Advances in Improving Stability of Food Emulsion by Plant Polysaccharides. *Food Res. Int.* **2020**, *137*, 109376. [CrossRef] [PubMed]
131. Lim, L.M.; Hadinoto, K. Enhancing the Stability of Amorphous Drug-Polyelectrolyte Nanoparticle Complex Using a Secondary Small-Molecule Drug as the Stabilizer: A Case Study of Ibuprofen-Stabilized Curcumin-Chitosan Nanoplex. *Int. J. Pharm.* **2020**, *575*, 119007. [CrossRef]
132. Shehzad, Q.; Rehman, A.; Jafari, S.M.; Zuo, M.; Khan, M.A.; Ali, A.; Khan, S.; Karim, A.; Usman, M.; Hussain, A.; et al. Improving the Oxidative Stability of Fish Oil Nanoemulsions by Co-Encapsulation with Curcumin and Resveratrol. *Colloids Surf. B Biointerfaces* **2021**, *199*, 111481. [CrossRef]
133. Sabjan, K.B.; Munawar, S.M.; Rajendiran, D.; Vinoji, S.K.; Kasinathan, K. Nanoemulsion as Oral Drug Delivery-A Review. *Curr. Drug Res. Rev.* **2019**, *12*, 4–15. [CrossRef]
134. Sultana, S.; Alzahrani, N.; Alzahrani, R.; Alshamrani, W.; Aloufi, W.; Ali, A.; Najib, S.; Siddiqui, N.A. Stability Issues and Approaches to Stabilised Nanoparticles Based Drug Delivery System. *J. Drug Target* **2020**, *28*, 468–486. [CrossRef]
135. Zhang, M.; Fan, L.; Liu, Y.; Huang, S.; Li, J. Effects of Proteins on Emulsion Stability: The Role of Proteins at the Oil–Water Interface. *Food Chem.* **2022**, *397*, 133726. [CrossRef]
136. Francke, N.M.; Bunjes, H. Drug Localization and Its Effect on the Physical Stability of Poloxamer 188-Stabilized Colloidal Lipid Emulsions. *Int. J. Pharm.* **2021**, *599*, 120394. [CrossRef]
137. Kong, L.; Jin, X.; Hu, D.; Feng, L.; Chen, D.; Li, H. Functional Delivery Vehicle of Organic Nanoparticles in Inorganic Crystals. *Chin. Chem. Lett.* **2019**, *30*, 2351–2354. [CrossRef]
138. Muhammad, D.R.A.; Sedaghat Doost, A.; Gupta, V.; bin Sintang, M.D.; van de Walle, D.; van der Meeren, P.; Dewettinck, K. Stability and Functionality of Xanthan Gum–Shellac Nanoparticles for the Encapsulation of Cinnamon Bark Extract. *Food Hydrocoll.* **2020**, *100*, 105377. [CrossRef]
139. Wang, X.; Li, M.; Liu, F.; Peng, F.; Li, F.; Lou, X.; Jin, Y.; Wang, J.; Xu, H. Fabrication and Characterization of Zein-Tea Polyphenols-Pectin Ternary Complex Nanoparticles as an Effective Hyperoside Delivery System: Formation Mechanism, Physicochemical Stability, and in Vitro Release Property. *Food Chem.* **2021**, *364*, 130335. [CrossRef] [PubMed]
140. Bonaccorso, A.; Russo, N.; Romeo, A.; Carbone, C.; Grimaudo, M.A.; Alvarez-Lorenzo, C.; Randazzo, C.; Musumeci, T.; Caggia, C. Coating Lacticaseibacillus Rhamnosus GG in Alginate Systems: An Emerging Strategy Towards Improved Viability in Orange Juice. *AAPS PharmSciTech* **2021**, *22*, 123. [CrossRef] [PubMed]
141. Alshawwa, S.Z.; Kassem, A.A.; Farid, R.M.; Mostafa, S.K.; Labib, G.S. Nanocarrier Drug Delivery Systems: Characterization, Limitations, Future Perspectives and Implementation of Artificial Intelligence. *Pharmaceutics* **2022**, *14*, 883. [CrossRef] [PubMed]
142. Wang, C.; Li, J.; Han, X.; Liu, S.; Gao, X.; Guo, C.; Wu, X. Silk sericin stabilized proanthocyanidins for synergetic alleviation of ulcerative colitis. *Int. J. Biol. Macromol.* **2022**, *220*, 1021–1030. [CrossRef]

143. Wang, X.; Gu, H.; Zhang, H.; Xian, J.; Li, J.; Fu, C.; Zhang, C.; Zhang, J. Oral Core-Shell Nanoparticles Embedded in Hydrogel Microspheres for the Efficient Site-Specific Delivery of Magnolol and Enhanced Antiulcerative Colitis Therapy. *ACS Appl. Mater. Interfaces* **2021**, *13*, 33948–33961. [CrossRef]
144. Xiao, M.; Wu, S.; Cheng, Y.; Ma, J.; Luo, X.; Chang, L.; Zhang, C.; Chen, J.; Zou, L.; You, Y.; et al. Colon-specific delivery of isoliquiritigenin by oral ediblezein/caseate nanocomplex for ulcerative colitis treatment. *Front. Chem.* **2022**, *10*, 981055. [CrossRef]
145. Sorasitthiyanukarn, F.N.; Muangnoi, C.; Ratnatilaka Na Bhuket, P.; Rojsitthisak, P.; Rojsitthisak, P. Chitosan/alginate nanoparticles as a promising approach for oral delivery of curcumin diglutaric acid for cancer treatment. *Mater. Sci. Eng. C* **2018**, *93*, 178–190. [CrossRef]
146. Joshi, A.; Soni, A.; Acharya, S. In Vitro models and ex vivo systems used in inflammatory bowel disease. *Vitr. Model.* **2022**, *1*, 213–227. [CrossRef]
147. Araújo, F.; Sarmento, B. Towards the characterization of an in vitro triple co-culture intestine cell model for permeability studies. *Int. J. Pharm.* **2013**, *458*, 128–134. [CrossRef] [PubMed]
148. Prezotti, F.G.; Boni, F.I.; Ferreira, N.N.; de Souza e Silva, D.; Campana-Filho, S.P.; Almeida, A.; Vasconcelos, T.; Gremião, M.P.D.; Cury, B.S.F.; Sarmento, B. Gellan Gum/Pectin Beads Are Safe and Efficient for the Targeted Colonic Delivery of Resveratrol. *Polymers* **2018**, *10*, 50. [CrossRef] [PubMed]
149. Silva, I.; Pinto, R.; Mateus, V. Preclinical Study in Vivo for New Pharmacological Approaches in Inflammatory Bowel Disease: A Systematic Review of Chronic Model of TNBS-Induced Colitis. *J. Clin. Med.* **2019**, *8*, 1574. [CrossRef] [PubMed]
150. Gao, X.; Li, J.; Pang, X.; Cong, K.; Jiang, C.; Han, B.; Gao, J.; Wang, Z.; Hu, J.; Wen, K.; et al. Animal Models and Pathogenesis of Ulcerative Colitis. *Comput. Math. Methods Med.* **2022**, *2022*, 1574. [CrossRef]
151. Luo, R.; Lin, M.; Zhang, C.; Shi, J.; Zhang, S.; Chen, Q.; Hu, Y.; Zhang, M.; Zhang, J.; Gao, F. Genipin-Crosslinked Human Serum Albumin Coating Using a Tannic Acid Layer for Enhanced Oral Administration of Curcumin in the Treatment of Ulcerative Colitis. *Food Chem.* **2020**, *330*, 127241. [CrossRef]
152. Zhang, C.; Wang, X.; Xiao, M.; Ma, J.; Qu, Y.; Zou, L.; Zhang, J. Nano-in-Micro Alginate/Chitosan Hydrogel via Electrospray Technology for Orally Curcumin Delivery to Effectively Alleviate Ulcerative Colitis. *Mater. Des.* **2022**, *221*, 110894. [CrossRef]
153. Zu, M.; Xie, D.; Canup, B.S.B.; Chen, N.; Wang, Y.; Sun, R.; Zhang, Z.; Fu, Y.; Dai, F.; Xiao, B. 'Green' Nanotherapeutics from Tea Leaves for Orally Targeted Prevention and Alleviation of Colon Diseases. *Biomaterials* **2021**, *279*, 121178. [CrossRef]
154. Li, L.; Cui, H.; Li, T.; Qi, J.; Chen, H.; Gao, F.; Tian, X.; Mu, Y.; He, R.; Lv, S.; et al. Synergistic Effect of Berberine-Based Chinese Medicine Assembled Nanostructures on Diarrhea-Predominant Irritable Bowel Syndrome In Vivo. *Front. Pharmacol.* **2020**, *11*, 1210. [CrossRef]
155. McCoubrey, L.E.; Favaron, A.; Awad, A.; Orlu, M.; Gaisford, S.; Basit, A.W. Colonic drug delivery: Formulating the next generation of colon-targeted therapeutics. *J. Control Release* **2023**, *353*, 1107. [CrossRef]
156. Nardelli, S.; Pisani, L.F.; Tontini, G.E.; Vecchi, M.; Pastorelli, L. MMX® technology and its applications in gastrointestinal diseases. *Therap. Adv. Gastroenterol.* **2017**, *10*, 545. [CrossRef]
157. Varum, F.; Freire, A.C.; Bravo, R.; Basit, A.W. OPTICORE™, an innovative and accurate colonic targeting technology. *Int. J. Pharm.* **2020**, *583*, 119372. [CrossRef] [PubMed]
158. Varum, F.; Freire, A.C.; Fadda, H.M.; Bravo, R.; Basit, A.W. A dual pH and microbiota-triggered coating (Phloral™) for fail-safe colonic drug release. *Int. J. Pharm.* **2020**, *583*, 119379. [CrossRef] [PubMed]
159. A Commercially-Proven Colon Targeted Drug Delivery System. Available online: https://healthcare.evonik.com/en/drugdelivery/oral-drug-delivery/oral-drug-delivery-technologies/sustained-colonic-delivery (accessed on 10 April 2023).